Inter-annual variations of surface currents and transports in the Sicily Channel derived from coastal altimetry

Fatma Jebri, Bruno Zakardjian, Florence Birol, Jerome Bouffard, Loïc Jullion, Cherif Sammari

AGU PUBLICATIONS

JGR

Journal of Geophysical Research: Oceans

RESEARCH ARTICLE

10.1002/2017JC012836

Interannual Variations of Surface Currents and Transports in the Sicily Channel Derived From Coastal Altimetry

Fatma Jebri[1,2,3,4,5], Bruno Zakardjian[1], Florence Birol[5], Jérôme Bouffard[6], Loïc Jullion[1], and Cherif Sammari[4]

[1]Mediterranean Institute of Oceanography, Université de Toulon, CNRS/INSU, IRD, UM 110, La Garde, France, [2]Mediterranean Institute of Oceanography, Aix Marseille Université, CNRS/INSU, IRD, UM 110, Marseille, France, [3]Université de Tunis El Manar, Ecole Nationale d'Ingénieurs de Tunis, Tunis, Tunisia, [4]Institut National des Sciences et Technologies de la Mer, Carthage Salammbô, Tunisia, [5]Laboratoire d'Etudes en Géophysique et Océanographie Spatiales, OMP, Toulouse, France, [6]Earth Observation Directorate, ESRIN/EOP GMQ Section, RHEA for European Space Agency, Italy

Key Points:
- A 20 year time series of coastal altimetry reveals interannual variability modes of the surface circulation in the Sicily Channel
- The variations of its volume transports are estimated with an empirical transport-like model
- Interannual variability results from the Atlantic waters inflow and modulations of the mesoscale activity in coupled or compensating ways

Correspondence to:
F. Jebri,
fatma.jebri@legos.obs-mip.fr and
fatma.jebry@gmail.com

Citation:
Jebri, F., Zakardjian, B., Birol, F., Bouffard, J., Jullion, L., & Sammari, C. (2017). Interannual variations of surface currents and transports in the Sicily Channel derived from coastal altimetry. *Journal of Geophysical Research: Oceans*, *122*. https://doi.org/10.1002/2017JC012836

Received 27 FEB 2017
Accepted 19 SEP 2017
Accepted article online 28 SEP 2017

Abstract A 20 year coastal altimetry data set (X-TRACK) is used, for the first time, to gain insight into the long-term interannual variations of the surface circulation in the Sicily Channel. First, a spectral along with a time/space diagram analysis are applied to the monthly means. They reveal a regionally coherent current patterns from track to track with a marked interannual variability that is unequally shared between the Atlantic Tunisian Current and Atlantic Ionian Stream inflows in the Sicily Channel and the Bifurcation Tyrrhenian Current outflow northeast of Sicily. Second, an empirical altimetry-based transport-like technique is proposed to quantify volume budgets inside the closed boxes formed by the crossing of the altimetry tracks and coastlines over the study area. A set of hydrographic measurements is used to validate the method. The inferred altimetry transports give a well-balanced mean eastward Atlantic Waters baroclinic flow of 0.4 Sv and standard deviations of 0.2 Sv on a yearly basis throughout the Sicily Channel and toward the Ionian Sea, which is fairly coherent with those found in the literature. Furthermore, the analysis allows to quantify the intrusions of Atlantic Waters over the Tunisian Shelf (0.12 ± 0.1 Sv) and highlights two main modes of variability of the main surface waters path over the Sicily Channel through the Bifurcation Atlantic Tunisian Current and Atlantic Ionian Stream systems. Some physical mechanisms are finally discussed with regards to changes in the observed currents and transports.

1. Introduction

The Sicily Channel (hereafter SC) plays a central role in the Mediterranean Overturning Circulation by controlling the water mass exchanges between the Eastern and Western subbasins of the Mediterranean and by linking their respective large-scale circulations. The water masses exchanges and flows between the two subbasins are, as first approximation, driven by a two-layer system: surface fresh Atlantic Waters (AW) flow eastward whereas more saline intermediate and bottom waters are formed in the eastern basin, i.e., the Levantine Intermediate Water (LIW) and the Eastern Mediterranean Deep Waters (EMDW), flowing westward (Astraldi et al., 1996, 1999). This dynamics of water masses is modulated by its regional mesoscale variations, wind forcing, mixing processes (e.g., Lermusiaux & Robinson, 2001; Manzella et al., 1988; Stansfield et al., 2003) and largely constrained by the complex topography of the SC (e.g., Astraldi et al., 1999; Napolitano et al., 2003). Several recent studies following the detection in the 1990s of the Eastern Mediterranean Transient (e.g., Roether et al., 2014) have highlighted the SC as a key area to follow major changes in the Mediterranean Overturning Circulation (e.g., Gasparini et al., 2005; Malanotte-Rizzoli et al., 2014).

We focus here on the surface circulation that regulates the AW path toward the Ionian Sea and Levantine basin. In the pioneering works, the AW was always considered flowing South East from Sicily toward the Libyan coasts (Lacombe & Tchernia, 1972; Nielsen 1912; Ovchinnikov, 1966). Recent studies using drifters (Poulain & Zambianchi, 2007), numerical simulations (Béranger et al., 2004) or coastal altimetry (Jebri et al., 2016) have depicted more complex circulation patterns (Figure 1a) with much of the AW feeding two main streams, the Atlantic Ionian Stream (AIS) flowing south-eastward close to Sicily (Buongiorno Nardelli et al., 2001; Robinson et al., 1999) and the Atlantic Tunisian Current (ATC) flowing southward over the Tunisian shelf (Sammari et al., 1999). The ATC may also have secondary currents branches over the Gulfs of Gabes

J_ID: JGRC Customer A_ID: JGRC22508 Cadmus Art: JGRC22508 Ed. Ref. No.: 2017JC012836 Date: 12-October-17 Stage: Page: 2

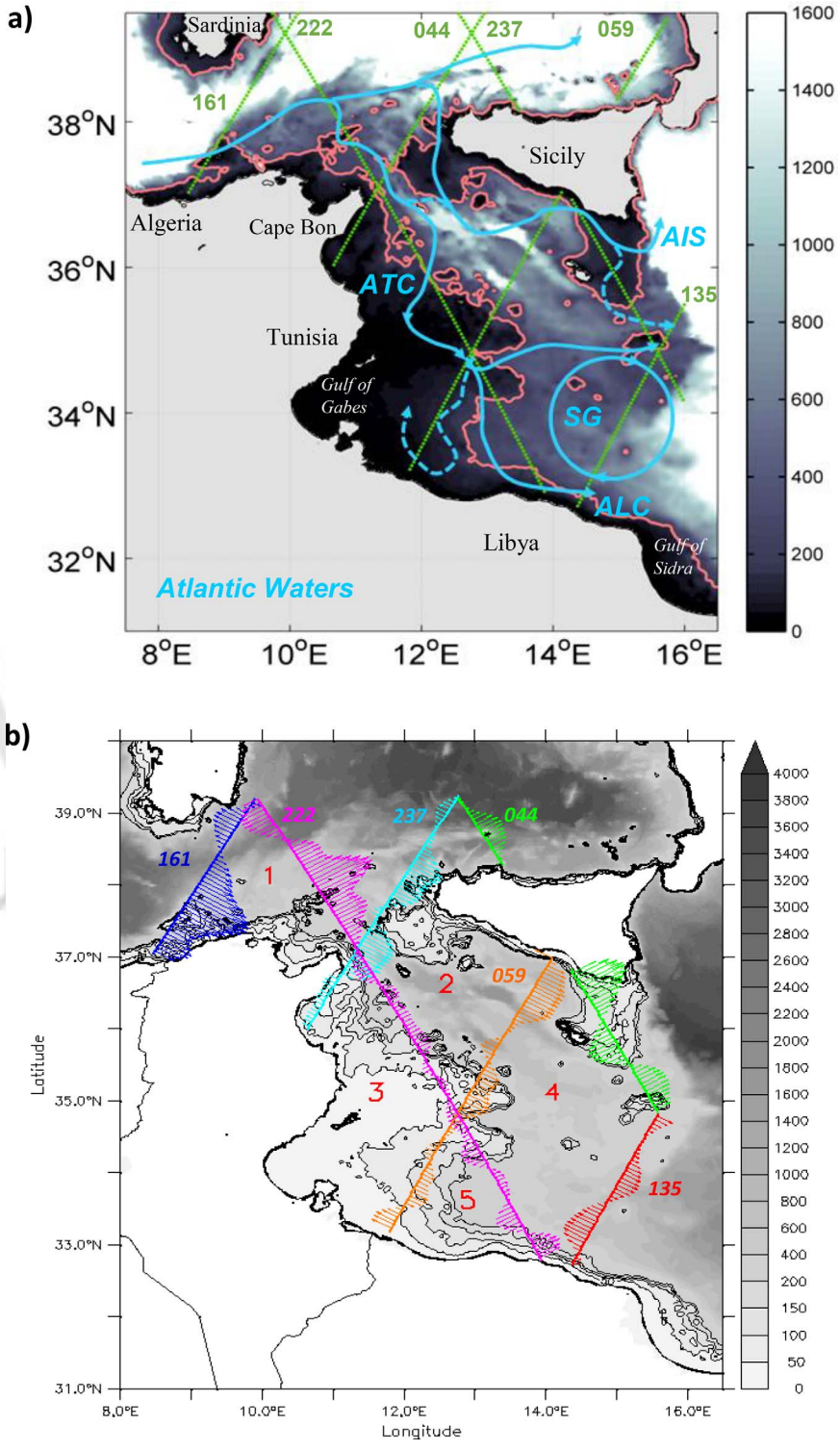

Figure 1. (a) Scheme of the main Atlantic waters circulation features at the upstream and over the Sicily Channel based on Jebri et al. (2016). Acronyms are listed in Table 1. The altimetry tracks (044, 059, 135, 161, 222, and 237) from the T/P + J1 + J2 mission and crossing the study area are shown in green dashed lines. The 200 m isobath (pink solid line) is from ETOPO2v1 global gridded database. (b) Mean absolute geostrophic cross-track velocities computed from the selected TP + J1 + J2 altimetry tracks over the period 1993–2013.

ID: kannanb Time: 13:09 I Path: //chenas03/Cenpro/ApplicationFiles/Journals/Wiley/JGRC/Vol00000/170402/Comp/APPFile/JW-JGRC170402

AGU Journal of Geophysical Research: Oceans 10.1002/2017JC012836

and Sidra, i.e., the Atlantic Libyan Current (ALC) (e.g., Jebri et al., 2016). This complex circulation has a marked seasonal component mainly driven by the AW transport seasonality, which is more intense in winter (November–February) and minimum in August (Gasparini et al., 2007; Manzella, 1994; Rinaldi et al., 2014). Recently, using 20 years of altimeter data and concurrent sea surface temperature images, Jebri et al. (2016) showed that the impact of the AW flow seasonality on the surface circulation of the SC results mainly in the strengthening of the ATC and ALC branches nearby and over the Tunisian shelf during winter.

Nevertheless, many questions still remain open about the interannual component of the SC surface circulation. Numerical modeling studies have mostly focused on a restricted part of the Central Mediterranean (e.g., Jouini et al., 2016; Pinardi et al., 1997), while sparse in situ based studies remain spatially limited to the SC entrance (e.g., Ben Ismail et al., 2012, 2014; Sammari et al., 1995) or to the northwestern part of the channel (e.g., Bonanno et al., 2014). The previous works of Buongiorno Nardelli et al. (1999, 2006) have demonstrated the potential of standard altimetry for the estimate of currents inside the SC. While long time series of reprocessed altimetry data are now available over the entire Mediterranean Sea, no attempt was yet made to study the interannual variability of the regional circulation in the SC from altimetry as it has been the case for other areas with narrow coastal boundary currents, such as the Liguro-Provençal Current in the North Western Mediterranean (Birol et al., 2010; Bouffard, 2007) and the Navidad current along the northern coast of Spain (Le Hénaff et al., 2011).

The main objective of this work, then, is to investigate the interannual variations of the surface circulation over the entire SC from a long-term (20 years) improved regional along-track altimetry data set recently developed and validated (Jebri et al., 2016). To this aim, the interannual variability of the altimetry-derived surface currents spatial is first documented through space/time diagram analysis. In a second time, the variability of the AW volume transports related to these surface current patterns is quantified using an empirical transport-like technique. This transport-like model is built by projecting cross-track geostrophic velocities at depth and assuming volume transport continuity through the closed boxes delimited by the crossing of the altimetry tracks and coastlines, including regional bathymetry constraints. The paper is organized as follows: the data set is presented in section 2. The interannual variations of the surface currents and transports both derived from altimetry are analyzed in sections 3 and 4, respectively. In section 5, we shed some light on the crucial questions and the potential causes of the interannual variability. Finally, a summary and some perspectives are given in section 6.

2. Material and Methods

2.1. Altimetry Data Set

For this study, we have first retrieved 20 years (1993–2013) of observations from the Topex/Poseidon, Jason-1, and Jason-2 altimetry missions (hereafter called T/P + J1 + J2) along six satellite tracks crossing the Central Mediterranean Sea (044, 059, 135, 161, 222, and 237; see Figure 1a). We used an experimental post-processed Sea Level Anomaly (SLA) altimetry product (X-TRACK) computed by the CTOH (Centre de Topographie des Océans et de l'Hydrosphère) and distributed by AVISO (http://www.aviso.altimetry.fr/en/data/products/sea-surface-height-products/regional/x-track-sla.html). The X-TRACK data are generated with a specific regional reprocessing algorithm improving the quality and availability of coastal altimetry data (e.g., Birol et al., 2010; Bouffard et al., 2011; Durand et al., 2008). The method details can be found in Roblou et al., (2011) or on the AVISO+ website. This altimetry product holds short spatial scale variations (along-track loess filter with a 40 km wavelength cutoff) and a high-resolution tidal correction derived from a regional version of the MOG2D model. It is noteworthy that no long wavelength error correction was used in X-TRACK to remove correlated noise due to orbit errors or uncertainties in geophysical corrections. Absolute Geostrophic Velocity (AGV) along the selected tracks is computed from the Absolute Dynamic Topography (ADT) following the method described in Jebri et al., (2016). We have computed the X-TRACK ADT by adding the regional Mean Dynamic Topography (MDT) (Rio et al., 2014) to the X-TRACK SLA. To minimize the noise impact when computing the across track AGV, we smoothed the ADT by the optimal filter of Powell and Leben (2004) at a four point size (i.e., 25 km) in accordance with the small baroclinic Rossby radius of deformation in the study area (∼15 km, Borzelli & Ligi, 1998). Such an optimal filter is expected to result in a slope noise standard deviation of 2–4 cm/s in the geostrophic velocity fields (Powell & Leben, 2004). For detailed information about the validation of the X-TRACK, data set over the study region please refers to Jebri et al.

J_ID: JGRC Customer A_ID: JGRC22508 Cadmus Art: JGRC22508 Ed. Ref. No.: 2017JC012836 Date: 12-October-17 Stage: Page: 4

AQ12AQ13

Table 1
Acronyms and Abbreviations

AC	Algerian Current
ADT	Absolute Dynamic Topography
AGV	Absolute Geostrophic Velocity
AIS	Atlantic Ionian Stream
ALC	Atlantic Libyan Current
ATC	Atlantic Tunisian Current
AVHRR	Advanced Very High Resolution Radiometer
AVISO	Archiving, Validation and Interpretation of Satellite Oceanographic Data
AW	Atlantic Waters
BATC	Bifurcation Atlantic Tunisian Current
BiOS	Bimodal Oscillating System
BTC	Bifurcation Tyrrhenian Current
CTD	Conductivity, Temperature, Depth
CTOH	Centre de Topographie des Océans et de l'Hydrosphère
EMDW	Eastern Mediterranean Deep Waters
EMT	Eastern Mediterranean Transient
LIW	Levantine Intermediate Water
MDT	Mean Dynamic Topography
MSSH	Mean Sea Surface Height
NAO	North Atlantic Oscillation
RMSE	Root Mean Square Error
SG	Sidra Gyre
SLA	Sea Level Anomaly
SST	Sea Surface Temperature
T/P+J1+J2	Topex/Poseidon, Jason-1 and Jason-2
SC	Sicily Channel

(2016). Here we only note that the estimated accuracy of altimetry-derived currents by comparison with 48 h moored current meter data of ~8 cm/s (see Jebri et al., 2016) is reduced to ~5 cm/s when the data sets are 90 days low-pass filtered (i.e., at interannual scale).

2.2. Ancillary Data

We use historical hydrographic data from SeaDataNet Pan-European infrastructure for ocean and marine data management (http://www.seadatanet.org/Data-Access/Common-Data-Index-CDI) to validate transport model parameters over the study area. Individual hydrographic profile went through standard data quality control procedures (http://www.seadatanet.org/Standards-Software/Data-Quality-Control). Several CTD casts are available on the SeaDataNet database for the area of interest (south of Sicily and long the Tunisian coasts). However, in our study only those collected on oceanographic cruises carried out on board the INSTM R/V Hannibal over the Sardinia Channel and the Tunisian shelf between 1995 and 2009 were used because we could not access to data from other line transect surveys. Note that most of measurements were sampled in spring and fall months. Winter data were available only during 1995, 1996, and 2009. More information about the sampling details of the oceanographic cruises (periods, number of casts, and stations) can be found in the SeaDataNet website or in Sammari et al. (1999) and Ben Ismail et al. (2014). Based on the classical dynamic method (Schilchtholz, 1991), the temperature and salinity fields of the available CTD data are used to compute the surface dynamic heights and estimate the in situ surface geostrophic currents, as in Ben Ismail et al. (2012, 2014), with a 320 m reference level for the deeper CTD casts (300 dbar in Buongiorno Nardelli et al., 1999, 2006) and the bottom depth for those on shallower bathymetry.

We also considered a sea surface temperature (SST) reprocessed product based on AVHRR Pathfinder Version 5.2 data set obtained from the Copernicus Marine Environment Monitoring Service (http://marine.copernicus.eu; technical@gos.artov.isac.cnr.it; Buongiorno Nardelli et al., 2013; Casey et al., 2010) and available from 1981 to 2012. This data set consists of regional, gap-free, Level 4 maps available daily at a high spatial resolution (1/24°) representative of night SST values. Monthly SST means are used in section 5 to provide complementary information on the surface currents.

ID: kannanb Time: 13:09 I Path: //chenas03/Cenpro/ApplicationFiles/Journals/Wiley/JGRC/Vol00000/170402/Comp/APPFile/JW-JGRC170402

AGU Journal of Geophysical Research: Oceans 10.1002/2017JC012836

Table 2
Percentage of the Explained Variance of the First Four EOF Modes for the Selected Parts of Altimetry Tracks

Track	Mode 1	Mode 2	Mode 3	Mode 4
161	32	20	13	7
222-North	21	19	12	10
044-North	46	17	13	9
237	15	13	12	8
059	22	19	12	10
222-South	25	14	8	7
044-South	23	21	11	10
135	28	16	13	11

Note. Track 044 is subdivided in two parts, north of Sicily (044-North) and south of Sicily (044-South). Same for track 222 with a part at the upstream of the SC (222-North) and the other inside the channel (222-South).

3. Interannual Variability of the Surface Currents

We start the analysis by investigating the oceanic surface variability in the study area from the monthly along-track AGV by using Empirical Orthogonal Function (EOF) analysis. The explained variance of the first modes ranges between 15% and 35% for all tracks, except for track 044-North with 46%, and is sometimes close to that of the second modes as the sum of the first four modes is varying from 49% to 71% (see Table 2). Due to this lack of clearly dominating spatial patterns for most of tracks, the analysis of the related current patterns may be ambiguous to interpret from track to track and preclude any synoptic view over the whole area. We then focus mainly on the temporal variability of the first four modes with Figure 2 presenting the energy spectra of the time series (principal components) of the four modes (grey lines) and their mean spectrum (black lines) for the different tracks. Except for track 135, the most energetic harmonic of the remaining tracks corresponds to the annual cycle (12–13 months) with a different energy level from one track to the other. The latter is markedly weaker downstream (tracks 135 and 237) than upstream of the channel (track 161). This annual frequency clearly dominates the most significant peaks at higher frequencies (e.g., at ~3–6 months) or the intermediate ones in the interannual band. Those are slightly above the subannual ones, but variable from one track to the other. Nevertheless, some common peaks at 4–5 (2.5–3) years are clearly seen on tracks 059, 044, and 135 (161, 222, and 044), but are generally of ambiguous significance level. Given the strong domination of the seasonal cycle, we applied a low-pass 12 months filter on the altimetry time series to extract specifically the interannual variations of the surface currents. The corresponding Hovmüller diagrams are shown in Figure 3. Note that track 222 which crosses all the TSC in northwest-southeast direction is split in three parts and interleaved between the other tracks to better illustrate the flows connection and continuity.

The first significant feature showed in Figure 3 is the cyclical burst within the Algerian Current (AC) core off the Algerian Tunisian shelf (track 161; 37.9°N−38.2°N) and eastward on the upper part of track 222. It shows velocities up to 25 cm/s on track 161 occurring almost every 2–3 years from 1993 to 2004, then over a continuous period from 2008 to 2011. These bursts are likely coherent with the energy peaks observed at 2–3 years on the spectrum of tracks 161 and 222 (Figure 2). This 2–3 years signal is less obvious on track 237 due to the split into a branch fluctuating toward the edge of the Northwest Sicilian coast, at the origin of the AIS/Bifurcation Tyrrhenian Current (BTC), and a second one following the continental slope of Cape Bon, and leading to the ATC. The latter accelerates (AGVs > 25 cm/s) around 37°N during 2001–2002, 2009, and 2012, but also meanders meridionally. The BTC on the upper part of track 044 shows coherent fluctuations with the AC (i.e., in the 2.5–3 years range), besides a significant tendency to enlarge and intensify from 2002 to 2013.

Eastward inside the SC, the northernmost part of tracks 059 and 044 exhibits a current vein corresponding to the AIS location, just southward of the Sicily coast, with a mean velocity exceeding 15 cm/s. On track 059, the AIS position shifts interannually from 36.25°N to nearby the Sicilian coasts (36.9°N) showing wider offshore expansions during 1999–2001, 2005, and 2009 likely due to the Sicily upwelling year to year variability (Bonanno et al., 2014). The AIS accelerates remarkably in 2001 reaching velocities greater than 25 cm/s. By contrast, we observe on track 044 an AIS constantly off the coast (~10 km) and flowing east toward the Ionian basin with a quasi-steady width (~70 km) and intensity, except in 2003 and 2011 where the current weakens significantly.

In the Southern part of the SC, the ATC flows south-eastward along the slope of the Tunisian shelf and splits into two branches around 35°N on track 059: one forming the Bifurcation Atlantic Tunisian Current (BATC) that continues eastward, and the other ultimately feeding the ALC which flows toward and along the Libyan coast. The ATC/ALC fluctuates every 3–5 years and shows weak velocities (5–10 cm/s). The BATC flows slightly northward with a weakly variable and smooth (5 cm/s) background vein, but reveals two marked intensifications (15–20 cm/s) accompanied by large extensions (35–35.5°N) in 2003 and 2011.

The ATC and BATC flows are less evident in the middle part of track 222 (33.5°N–36°N) due to its along slope, and hence along the main current, orientation. The ATC signature in the middle part of track 222 is a southwestward vein flowing onto the shelf near Cape Bon (~37°N) with weak velocities (~5 cm/s) all over

J_ID: JGRC Customer A_ID: JGRC22508 Cadmus Art: JGRC22508 Ed. Ref. No.: 2017JC012836 Date: 12-October-17 Stage: Page: 6

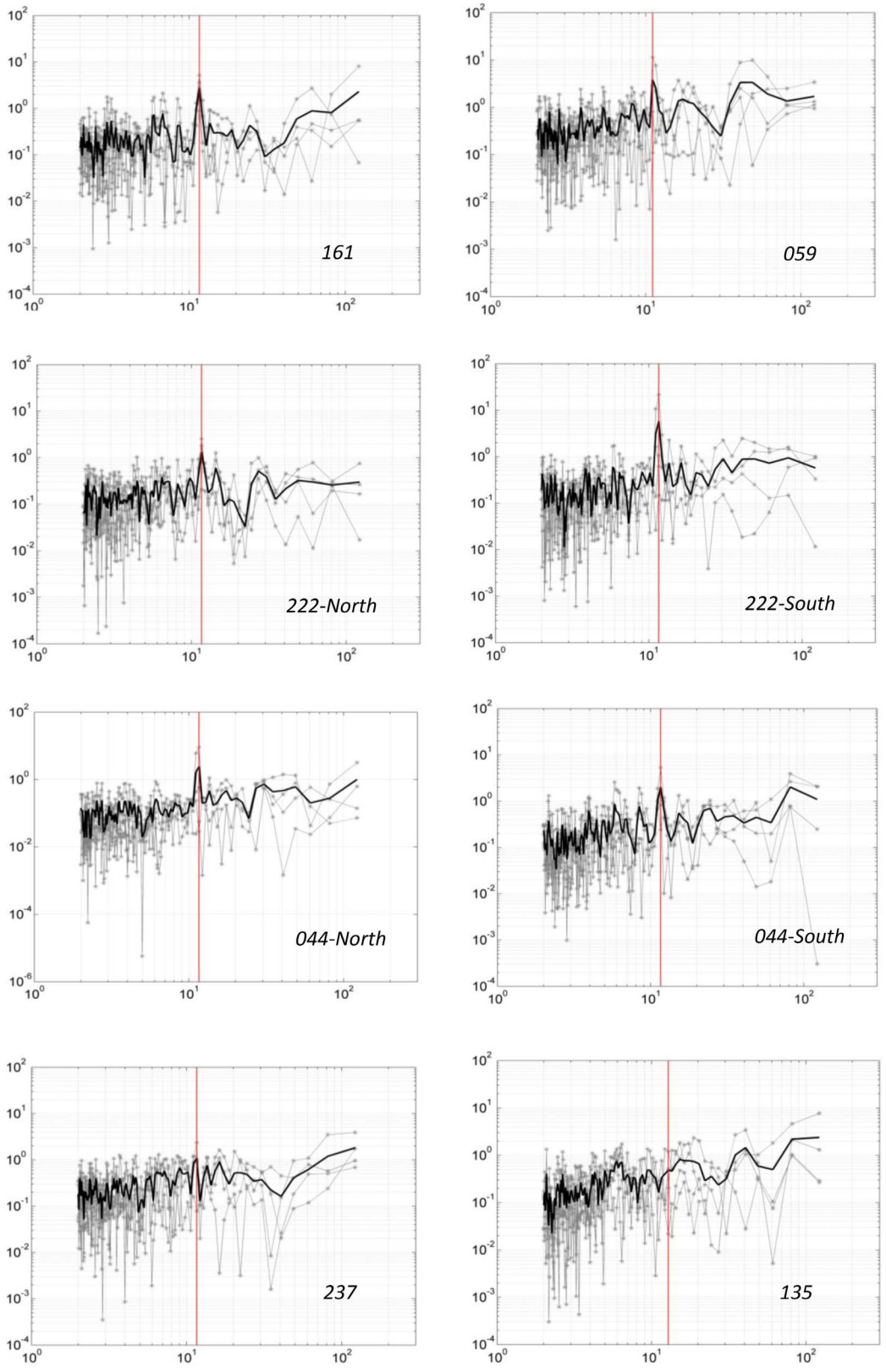

Figure 2. Spectrum of the time series associated to the first four EOF modes of the monthly cross-track absolute geostrophic current for the selected TP + J1 + J2 altimetry tracks. The individual spectrums of each track point are shown in grey line and the mean spectrum is presented in black. The red vertical lines indicate the annual harmonics. Track 044 is subdivided in two parts, north of Sicily (044 North) and south of Sicily (044 South). Same for track 222 with a part at the upstream of the SC (222 North) and the other inside the channel (222 South).

ID: kannanb Time: 13:10 I Path: //chenas03/Cenpro/ApplicationFiles/Journals/Wiley/JGRC/Vol00000/170402/Comp/APPFile/JW-JGRC170402

AGU Journal of Geophysical Research: Oceans 10.1002/2017JC012836

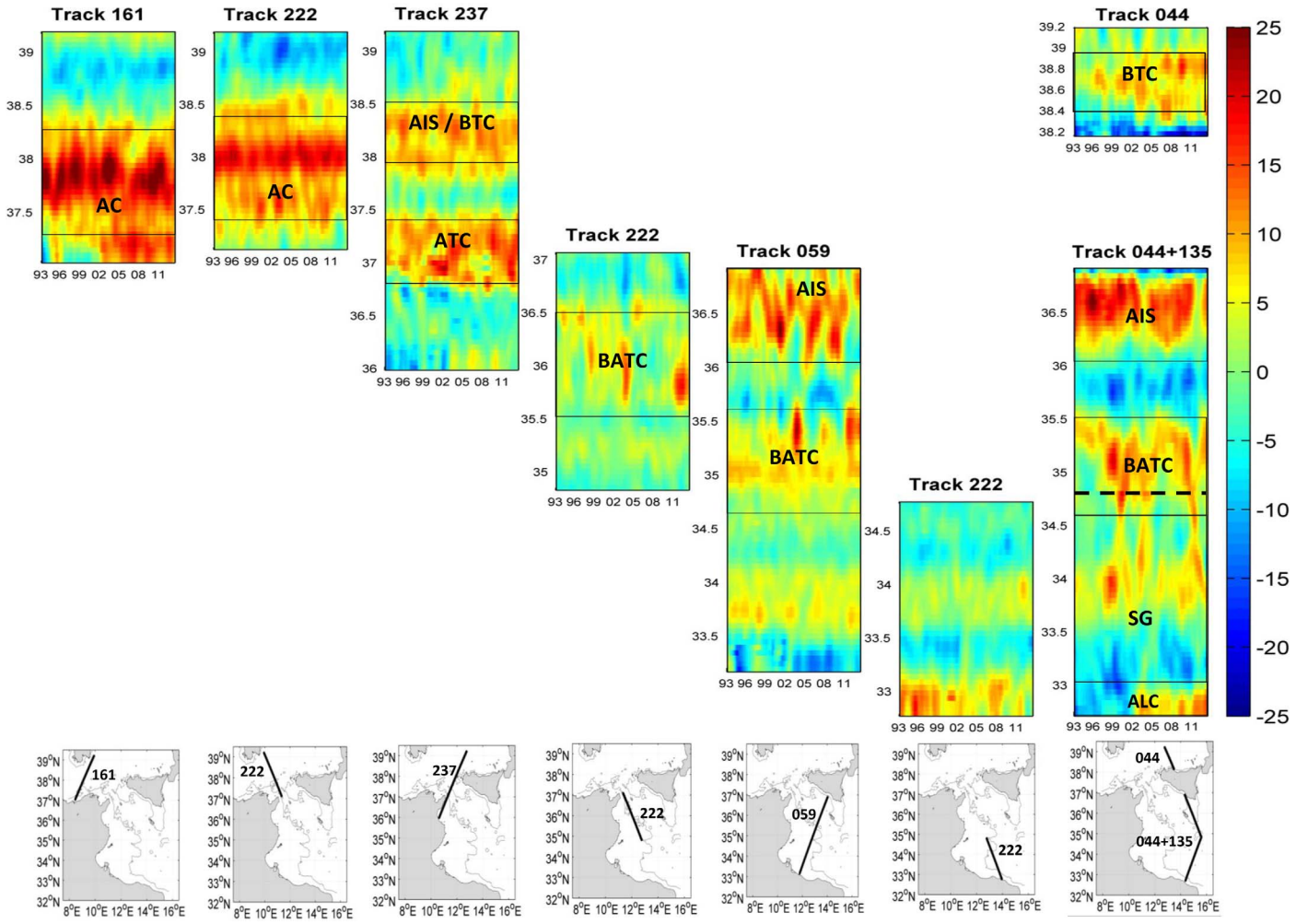

Figure 3. (top) Hovmöller diagrams of the 12 months filtered cross-track geostrophic velocities (bottom) for each of the selected tracks or part of tracks. The different tracks are ordered in longitude and over the same latitude scale in order to highlight flow continuation between the different current veins from the westernmost track (161) at the entry of the SC to the easternmost ones (135-044) at its exit. The main currents positions are shown on each Hovmöller (see black thin lines). Acronyms are listed in Table 1. The dashed thick line on 044 + 135 plot indicates the edge between the two adjacent tracks 044 and 135.

the 20 year period, except for 2003 and 2011 where it shows evidence of higher velocity (∼15 cm/s). Over the Gulf of Hammamet, (∼35.7°N–36.7°N) the flow reverses eastward with positive velocities particularly high (15 cm/s) during 2003 and 2011 and jointly with the two marked events previously seen on track 059 and attributed to the increased BATC flow. Further south on track 222 (∼33.1°N–35.5°N), the along-slope branch of the ATC fluctuates in east-west motions with relatively homogeneous intensity throughout the years (∼5–8 cm/s), except for 2011 where it reaches a maximum of 13 cm/s around 33.7°N. The remaining vein at latitudes southward of 33.2°N has a dominant eastward direction and likely corresponds to the ALC that holds for the final exit for the Tunisian shelf AW flow, constrained by the Libyan coast to a narrow coastal jet.

The BATC continuation toward the East on track 044 + 135, between 35.5°N and 36°N, shows higher velocities and even more marked fluctuations likely due to an undulating recirculation from the upper AIS or westward flow from the Ionian Sea. On the contrary, the 2003 and 2011 events are reminiscent of the previous anomalies seen on tracks 059 and 222. The coherency of these, jointly with increased AC on track 161 and the weakening of the AIS on track 044, ultimately suggest major changes of the main AW (ATC/BATC versus AIS) pathways toward the Ionian Sea. We note that the most pronounced BATC fluctuations lead to flow interactions with the northern eastward flow of the Sidra Gyre (SG), especially in 2000, 2003, and 2011.

J_ID: JGRC Customer A_ID: JGRC22508 Cadmus Art: JGRC22508 Ed. Ref. No.: 2017JC012836 Date: 12-October-17 Stage: Page: 8

However, this does not seem to strongly affect the SG interannual variability whose significant intensification is rather observed, during 1998–1990 and between 2006 and 2010, mainly on its southeastern branch.

Last, the southern part of track 135 shows a clear regime shift after 2002 with an eastward coastal current, likely corresponding to the ALC that seems to appear suddenly, jointly with an AC increase and extent southward very closely to the coastline on track 161. This shifting period coincides with a technology change between the end of TOPEX/Poseidon and the launch of Jason-1 missions, which would cause some large wavelength bias. However, the bias associated with the change of MSSH (Mean Sea Surface Heights) used to generate TOPEX/Poseidon and Jason-1 X-TRACK is of the order of millimeters and thus would not significantly affect the sea level gradients used for AGV calculations. This hints at a dynamical mechanism rather than an instrumental error as the most plausible cause for this signal. However, the altimetry time series is too short (23 years) to draw any significant conclusion on the potential mechanism underpinning this decadal variability.

4. Transport-Like Analysis

The cross-track currents derived from the altimetry data (AGVs) provide valuable yet qualitative information on the surface circulation, mainly the AW flow and its associated pathways, and show significant spatial coherence in the interannual variability. This methodology has two main caveats. First, the AGV is only a component of the total current. Second, the velocities on the different tracks are not quantitatively comparable due to their different orientations (AVG projection) with respect to the dynamic patterns. Finally, the bathymetric variations along and between the different tracks are very high, ranging from $<$100 m near the coast and on the Tunisian shelf to about 500 m and down to 1,000–2,000 m in the central and the easternmost parts of the studied area, respectively.

In order to provide a more quantitative view of the regional circulation of the SC while ensuring that current structures are coherent regarding the continuity of the flows, we take advantage of the spatial layout of the altimetry tracks which, together with the coastlines delimit closed boxes (see Figure 1b). Since the AGV are normal to their associated tracks (and obviously are null when normal to the coastline), we can establish transport budget within these boxes. To do so, we defined a "proxy" for the AW transport (surface flow) based on the monthly means of the 20 years cross-track AGV, including bathymetric limitations on shallow area, that is used to estimate transport budget in each box. Thus, this is not an attempt to estimate true transports, but rather a quantitative diagnostic to assess the flow continuity between the different currents veins seen on each track and how the related interannual variability may significantly affect the main AW pathways over the study area. The model's assumption and formulation are described in the following section.

4.1. Model Equations and Tuning

Building on the work of Han and Tang (2001), the total volume transport (T) is the sum of the barotropic (T_{BT}), baroclinic (T_{BC}), and Ekman transport (T_E). The altimeter-derived current velocities obtained from along-track ADT assuming geostrophy (Bouffard et al., 2008; Jebri et al., 2016) are not thought to include the Ekman component of the surface circulation, which must be treated apart. More, the Ekman transport concerns only the first meters of the surface layer and its impact should be insignificant in comparison to that of the geostrophic transport (e.g., Bouffard et al., 2010). Nevertheless, it will be discussed later. The main part of the high-frequency ($<$10 days) component of the barotropic signal forced by pressure is removed from the altimetry data through a regional version of the tide model Mog2D. Though altimetry signal may still contain the lower frequency barotropic signal due to wind forcing, Rintoul et al. (2002) and Buongiorno Nardelli et al. (2006) suggested that it rather retains the baroclinic part of the geostrophic circulation. In practice, density data are required in addition to the altimetric velocities to quantify properly the barotropic and the baroclinic transports (e.g., Fofonoff, 1962; Han & Tang, 2001). Buongiorno Nardelli et al. (2006) have extrapolated to depth the geostrophic velocities along a Topex/Poseidon track crossing the SC for three particular dates, using simultaneous hydrographic measurements and a statistical approach. Though their method is robust and very promising for the monitoring of currents variability, it surely requires a continuous in situ survey along the altimetry tracks. This high sampling of in situ data is rarely available over the SC, in particular on the Tunisian and Libyan shelves.

ID: kannanb Time: 13:10 I Path: //chenas03/Cenpro/ApplicationFiles/Journals/Wiley/JGRC/Vol00000/170402/Comp/APPFile/JW-JGRC170402

J_ID: JGRC Customer A_ID: JGRC22508 Cadmus Art: JGRC22508 Ed. Ref. No.: 2017JC012836 Date: 12-October-17 Stage: Page: 9

In the case of the Sicily Strait, the LIW and AW flows being opposite, there is a no motion layer signing their interface as shown in Buongiorno Nardelli et al. (2006). Assuming this AW/LIW interface as a reference depth, any projection of surface velocity values down to it should be able to reproduce grossly the baroclinic component of the AW related flow. This hypothesis is equivalent to considering a positive value as a net AW eastward transport (over the LIW westward one). Negative values may be representative of westward recirculations of the AW flow or possibly of mixed AW with Ionian sea surface Waters (i.e., Modified AW) or Western Intermediate Waters (e.g., Ben Ismail et al., 2014). Here our transport-like model is simply defined as the double integral along a track and down to a reference depth of a projected depth-dependent geostrophic current ($U_g(x,z)$) defined as:

$$T = \int_{x_0}^{x_{end}} \int_{0}^{Z_{max}} U_g(x,z)\,dx\,dz \tag{1}$$

where x_0 and x_{end} stand for the start and end of each part of a track so that a "track-closed-box" is formed. Z_{max} is the reference depth of integration, adjusted to bathymetry (derived here from the global "Etopo01" data set) in the shallow portion of the track (i.e., when Z_{bathy} is less than Z_{max}). The distribution of the geostrophic current with depth is defined, from the altimetry AGV, assuming an exponential-like (secant hyperbolic) depth-dependency:

$$U_g(x,z) = AVG(x) \times [sech(\lambda(x) \times z)] \tag{2}$$

$$\text{where} \lambda(x) = \frac{sech^{-1}(0.01)}{\min(Z_{max}, Z_{bathy}(x))} \tag{3}$$

so that the retained baroclinic component is reduced to 1% of the surface velocity at depth Z_{max} or adjusted to the local bathymetry, when Z_{max} is deeper than the local bottom depth Z_{bathy}. The use of a secant hyperbolic gave a reasonably good fit with the shapes of observed baroclinic profile as shown for the example of November 1996 in Figure 4, comparing the analytical profiles derived from the altimetry AVG on track 237 F4 with the observed profiles from the CTD velocities on Transect "SI." Some preliminary tests with a linear function and an exponential one simply showed higher and lower, respectively, geostrophic currents at middepths due to change in the depth decay, and hence transports. However, they did not change significantly the relative importance of the simulated transports nor the order of magnitude of residuals in each box.

The most delicate issue is the definition of a meaningful water mass boundaries between the surface (AW and Modified AW) and the intermediate (LIW) layers, given the many different water masses crossing the area and that the vertical extent of structures related to the AW flow in the Sardinia-Tunisia-Sicily area is not homogeneous (e.g., Ben Ismail et al., 2014; Buongiorno Nardelli et al., 2006; Onken et al., 2003). The main AW current vein at the Channel of Sardinia has a vertical extension ranging around 150–200 m (e.g., Astraldi et al., 1999; Onken et al., 2003; Sammari et al., 1995). It is reduced inside the SC (11°E–13°E; 36.5°N–37.8°N) where the LIW counterflow at depth limits more the vertical extension of the AW flow. The interface between the two opposite flows is not homogenous and is often defined by a salinity range of 37.8–38.2, depending on authors, as between ~100 and 150 m depth (e.g., Astraldi et al., 1996; Grancini & Michelato, 1987; Onken et al., 2003; Sammari et al., 1995). An AW/LIW interface depth of ~125 m was also observed in (Gasparini et al., 2004) from current meter measurements. Considering as much as possible the distribution of the different water masses present in the area, this interface (i.e., Z_{max}) cannot be fully defined for each month and each track over a 20 years period. So, we first set up the Z_{max} values at 200 m upstream and 125 m inside the SC based on the above literature. We secondly made some sensitivity tests, mainly for Z_{max} value inside the SC (100, 125, 150, and 200 m) as illustrated in Table 3. These tests showed logically an T3 increase (decrease) of the associated volume transports for deeper (lower) *Zmax* on most of the cross-track sections (i.e., the deepest ones), but did not change qualitatively the relative strengths of the main current veins (i.e., ALC, BATC, AIS, etc.). For instance, for track 222 south of Sicily, the increase varies from 0.005 to 0.01 Sv as the Z_{max} deepen from 125 to 150 or 200 m. The associated residuals of the volume transports for each box were slightly affected, except a marked degradation for the 200 m value of about 0.1 and 0.05 Sv for boxes 2 and 5, respectively (see Table 3). Lastly, the Z_{max} parameter was set then at 200 m west ($<$11.30°E) and at 125 m inside ($\geq$11.30°E) of the SC as these values gave the better long-term residuals for most of the boxes.

ID: kannanb Time: 13:10 I Path: //chenas03/Cenpro/ApplicationFiles/Journals/Wiley/JGRC/Vol00000/170402/Comp/APPFile/JW-JGRC170402

AGU Journal of Geophysical Research: Oceans 10.1002/2017JC012836

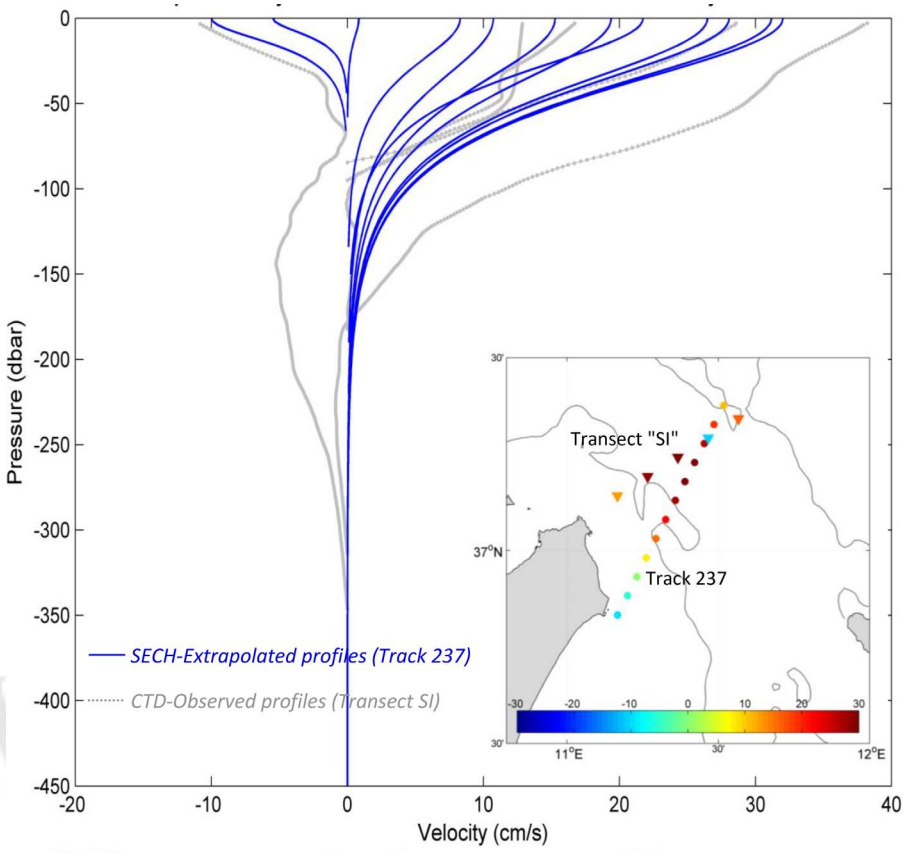

Figure 4. Example of altimetry vertical profiles extrapolated with a secant hyperbolic velocity function (solid blue lines) for track 237 on 4 November 1996 against observed CTD vertical velocity profiles (dotted grey lines) for a Sicily transect (SI) on 5 November 1996. The location of both transects is superimposed on the map at bottom right.

Table 3
Sensitivity Tests Carried Out for the Z_{max} Parameter Upstream (Z_{max}-North) and Inside (Z_{max}-South) the Sicily Channel of the Secant Hyperbolic Velocity Function

Z_{max} Setting (m)					
Z_{max}-North	200	200	200	200	250
Z_{max}-South	100	125	150	200	125
Tracks Transports (Sv)					
161	0.8306	0.8306	0.8306	0.8306	0.9543
222-North	0.7000	0.7000	0.7000	0.7000	0.8612
237	0.6749	0.6749	0.6749	0.6749	0.8173
044-North	0.2239	0.2239	0.2239	0.2239	0.2799
222-South	−0.0272	−0.0353	−0.0402	−0.0522	−0.0353
059	0.3739	0.4413	0.5072	0.6326	0.4413
044-South	0.2710	0.3527	0.4121	0.4658	0.3527
135	0.0122	0.0148	0.0168	0.0197	0.0148
Boxes Transports (Sv)					
Box 1	0.0139	0.0139	0.0139	0.0139	−0.0348
Box 2	0.0581	0.0020	−0.0549	−0.1693	0.0771
Box 3	0.0189	0.0075	−0.0012	−0.0123	0.0188
Box 4	−0.0342	−0.0706	−0.0799	−0.0341	−0.0706
Box 5	0.1249	0.1443	0.1581	0.1812	0.1443

Note. The associated transports values for the different tracks and their residuals inside the closed boxes are also shown. Track 044 is subdivided in two parts, north of Sicily (044-North) and south of Sicily (044-South). Same for track 222 with a part at the upstream of the SC (222-North) and the other inside the channel (222-South).

J_ID: JGRC Customer A_ID: JGRC22508 Cadmus Art: JGRC22508 Ed. Ref. No.: 2017JC012836 Date: 12-October-17 Stage: Page: 11

4.2. Model Validation Using Independent In Situ Estimates

We test the transport-like model first by comparing the geostrophic velocity profiles estimated from altimetry with those from available simultaneous hydrographic measurements made over the Tunisia-Sardinia sections ("SA1, SA2, and SA3") versus tracks 161 and 222 and the Tunisia-Sicily section ("SI") versus track 237. Figures 5 and 6 show examples of such comparisons for November 1996, July 2006, and July 2007. Globally, all sections show an upper layer with a coastal jet marked by high eastward velocities (>20 cm/s) corresponding to the core of the AW as defined by the in situ salinity profiles (not shown). The eastward AW vein on the "SA1," SA2, and "SA3" sections loosely agrees with that derived from altimetry on tracks 161 or 222, respectively, regarding its position with respect to the bathymetry slope and its intensity. The vertical structures extrapolated from altimetry give velocities slightly weaker than those derived from the CTD fields, mainly due to the smoothing effect of the secant hyperbolic function. Hence, the depth extension of the current seems to be slightly lower (by ~30 m), especially in November 1996, and the interface with the intermediate layer (i.e., the zero velocity isoline) is unclear on the altimetry sections. Further east, the "SI" section, close to track 237, shows an in situ derived eastward geostrophic current of 25–30 cm/s with a maximum depth extension of 150 m and a marked mesoscale variability that is not reproduced by the monthly averaged altimetry-derived AGV. Likewise, the in situ geostrophic currents of the "SI" section highlight a well-defined LIW/AW interface and even *westward* LIW veins at depth (> 150 m), especially in July 2006. Nevertheless, the vertical structure of the upper layer derived from these tracks is globally coherent with that of the in situ derived geostrophic current.

There are a number of factors that can cause the altimeter AGV to differ from the in situ currents. As such, their lack of colocation, as the available CTD transects are not always in the best configuration regarding the orientation of the altimetry tracks. Observed discrepancy can also be explained by the lack of synopticity of the CTD data. As such, an uncompleted resolution of the temperature and salinity gradients and hence of the density ones, or the time shift between the in situ measurements and the altimeter passage. This time shift between both estimates varies from few hours to 4 days in our case (see Figures 5 and 6), and the larger it gets, the most significant differences are noted. This time shift would be particularly constraining such comparisons in an area of marked mesoscale variability like the Central Mediterranean Sea (e.g., Buongiorno Nardelli et al., 2001, 2006).

Last, Figure 7 compares the corresponding estimates of the baroclinic transport over the upper 200 m depth. Despite the different locations, estimates of transports derived from both data fields give relatively good qualitative matches for the same months, even if in situ estimate are generally in the lower range of altimetry-derived values, likely due to differences in the spatial extent of the sampled sections between both estimates. The Root Mean Square Error (RMSE) is 0.415 Sv (0.291) Sv between the "SA1"("SI") sections and track 161 (237). The comparison of "SA2" to track 222 transports (dashed lines) resulted in a RMSE slightly higher by 0.027 Sv than that with track 161. Note that the "SI" transect is by far the most sampled transect among the available hydrographic data, which would explain its lower RMSE with altimetry compared to the few samples available for "SA1" and "SA2."

We were not able to apply the same analysis eastward inside the Sicily Channel due to the lack of adequate CTD data coverage. Indeed, the scarcer available CTD data are limited to transects over the Gulf of Hammamet with a southwest-northeast direction, thus perpendicular to the closest track (222). However, those generally show small or poorly resolved geostrophic structures with a limited vertical extension (not shown) of no more than 100–150 m over deeper area. Thus, we rely on the literature (see above) to define an interface depth (Z_{max}) of 125 m, for the calculation of the baroclinic AW transport for all tracks east of Cape Bon (>11.30°E).

4.3. Mean Box Transport Budget and Related Errors

The mean AW transport estimates based on the retained configuration are shown in Figure 8 with long-term averaged flow residuals calculated as the difference between the inflow and outflow of each track-closed box. Except for boxes 4 and 5, the long-term averaged flow residuals are significantly lower than the transports at their frontiers, not exceeding 12% of the boundary transports. This suggests that the long-term mean AGV has a spatial coherency that is conserved with this transport-like approach, despite the complex bathymetry of the area. For box 1, the estimate over the Sardinia Channel (track 161; >37°N) is

ID: kannanb Time: 13:10 I Path: //chenas03/Cenpro/ApplicationFiles/Journals/Wiley/JGRC/Vol00000/170402/Comp/APPFile/JW-JGRC170402

J_ID: JGRC Customer A_ID: JGRC22508 Cadmus Art: JGRC22508 Ed. Ref. No.: 2017JC012836 Date: 12-October-17 Stage: Page: 12

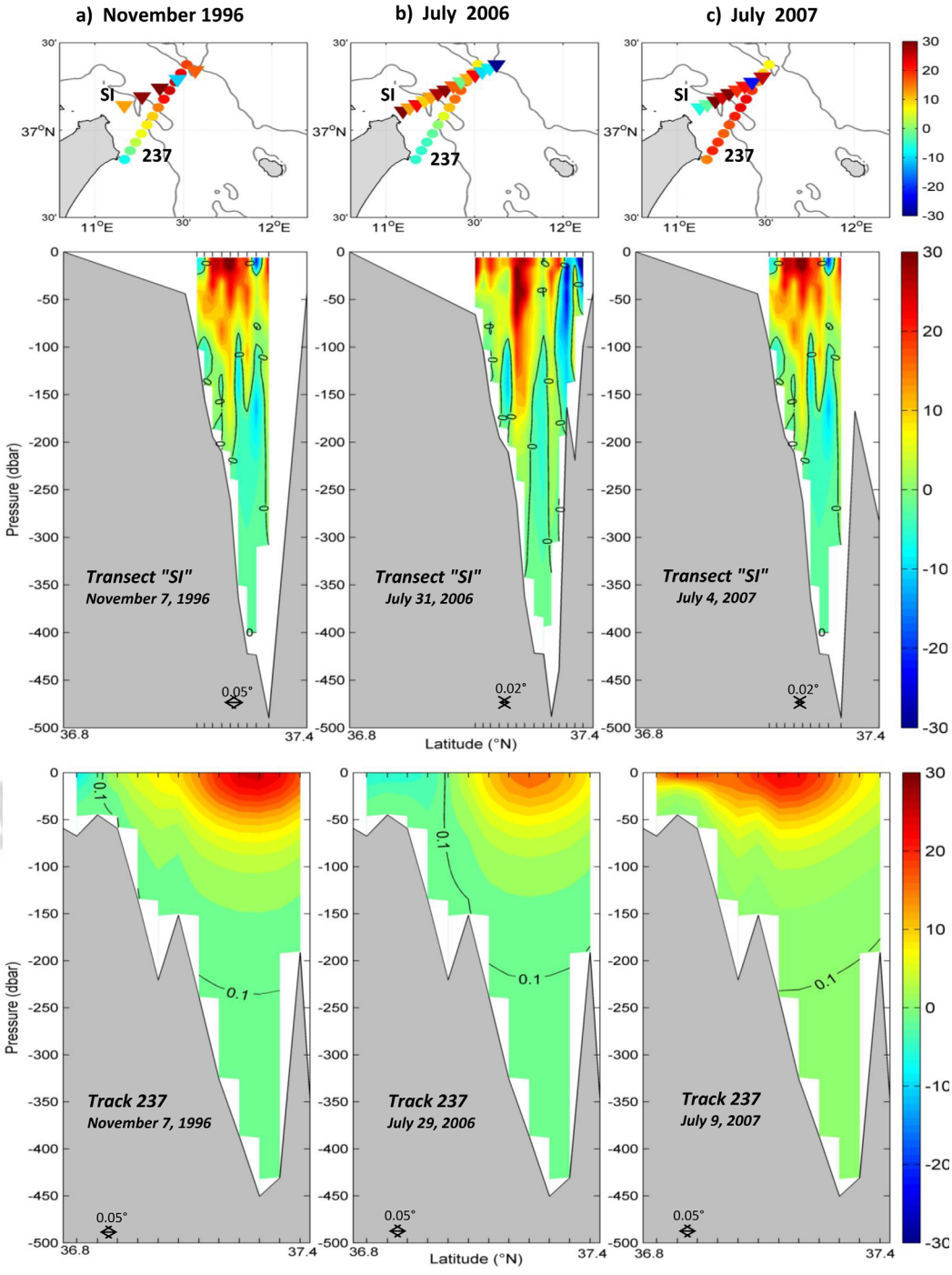

Figure 5. Comparisons between altimetry tracks (222 and 161) and CTD Sardinia transects (SA1, SA2, and SA3) geostrophic currents for (a) November 1996, (b) July 2006, and (c) July 2007. The surface patterns are shown on the top. (bottom) The vertical sections of the CTD (altimetry) transects are shown on the middle. The vertical sections of altimetry data are extrapolated from the theory "Sech" model (see equation (2)). Positive (negative) currents (in cm/s) indicate an eastward (westward) direction. The grey areas show the bathymetry, extracted from ETOPO2v1 global gridded database, for each point. The zero current value is indicated with a continuous black line. The time of passage of altimetry tracks and the day of measurement of CTD data are indicated on each vertical section.

0.83 Sv on average, from which 0.70 Sv continues eastward through track 222 (>37°N) while a small amount (0.12 Sv) enters the SC close to Cape Bon (southernmost part of track 237). These transport estimates led to a low mean residual (0.0139 Sv).

ID: kannanb Time: 13:10 I Path: //chenas03/Cenpro/ApplicationFiles/Journals/Wiley/JGRC/Vol00000/170402/Comp/APPFile/JW-JGRC170402

J_ID: JGRC Customer A_ID: JGRC22508 Cadmus Art: JGRC22508 Ed. Ref. No.: 2017JC012836 Date: 12-October-17 Stage: Page: 13

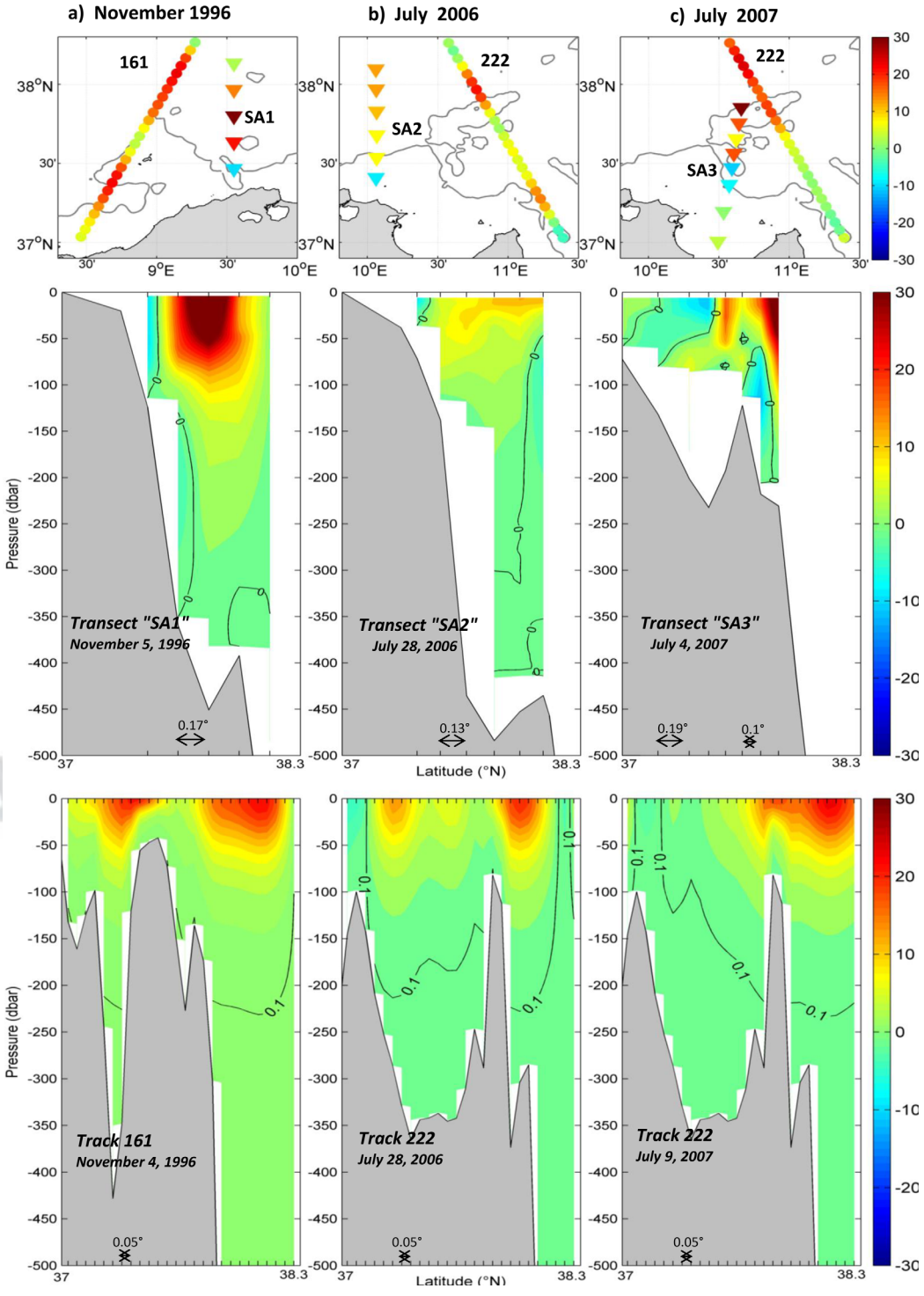

Figure 6. Same as Figure 4 but with the in situ Sicily transects (SI) against track 237.

The mean baroclinic AW transport inside box 2 (track 237; >37°N) is 0.56 Sv, from which 0.22 Sv escapes northwest of Sicily via the BTC (northern part of track 044) that is rather a mixture of AW and LIW (see Onken et al., 2003). Box 2 is also fueled by a small input from the Tunisian Shelf (0.0659 Sv, middle part of track 222), giving a total AW entering flow of 0.4 Sv. This AW transport entering the central SC is well balanced (residual of 0.0021 Sv) by a quasi-equivalent south-eastward transport of 0.39 Sv through the upper part of track 059 that combines the AIS and BATC flows. Box 3, which covers mainly the Tunisian shelf, also

ID: kannanb Time: 13:10 I Path: //chenas03/Cenpro/ApplicationFiles/Journals/Wiley/JGRC/Vol00000/170402/Comp/APPFile/JW-JGRC170402

J_ID: JGRC Customer A_ID: JGRC22508 Cadmus Art: JGRC22508 Ed. Ref. No.: 2017JC012836 Date: 12-October-17 Stage: Page: 14

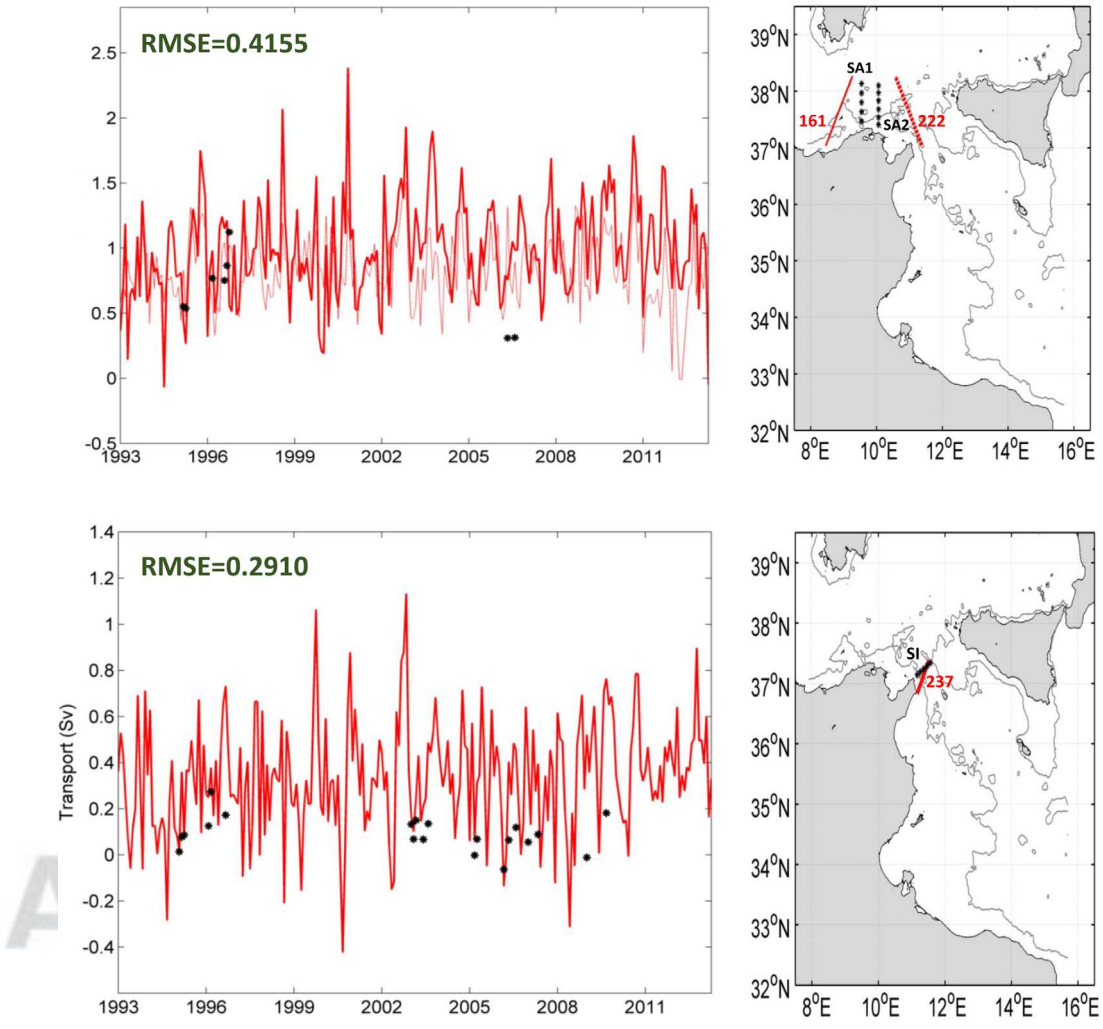

Figure 7. Comparison of transport times series estimates from altimetry tracks 161 and 222 with those (top) from CTD "SA1" and "SA2" transects and (bottom) from track 237 versus "SI" transects over the period 1993–2013.

shows a well-balanced mean flow budget with 0.12 Sv of AW inflow close to Cape Bon (from box 1) equally shared between its eastern (track 222; 0.0659 Sv toward box 2) and southern (track 059; 0.0632 Sv toward box 4) boundaries.

Box 4 shows a slightly reduced mean AW transport residual with a deficit of −0.071 Sv due to a weak (∼0.09 Sv) outflow across track 135 against 0.35 Sv outflow from track 044 south of Sicily, which is likely enhanced by the mean AIS and BATC flows from box 2. Box 5 holds by far the highest error (0.1444 Sv) due to both flows from the southernmost parts of tracks 059 and 222 that converges almost constantly with quasi-equivalent transports. The mean residual of box 5 (Tunisian Libyan shelf) contrast sharply with that of box 3 (Gulfs of Gabes and Hammamet), which is one of the best inside the channel despite being on a shallow-water shelf. In addition, the residual error of box 4 is very close to the southwestward transport of track 222 in box 5 which seems to be the main cause to its deficit. We noted previously (section 3) on the interannual current patterns of the southernmost part of track 135, an absence of the ALC signature before 2002 and a sudden appearance just afterward. By contrast, it is present all over the 20 years period in terms of transport at the southernmost part of track 222, but with intermittency and a tendency to decrease during the last decade. A box transport budget solely over the 2003–2013 period gives better results regarding box 4 residuals (with an inflow of AW of 0.42 Sv upstream track 059 and an outflow of 0.4 Sv downstream across tracks 135 and044), but without improving the box 5 "bad" residual. This suggests (though carefully)

ID: kannanb Time: 13:10 I Path: //chenas03/Cenpro/ApplicationFiles/Journals/Wiley/JGRC/Vol00000/170402/Comp/APPFile/JW-JGRC170402

J_ID: JGRC Customer A_ID: JGRC22508 Cadmus Art: JGRC22508 Ed. Ref. No.: 2017JC012836 Date: 12-October-17 Stage: Page: 15

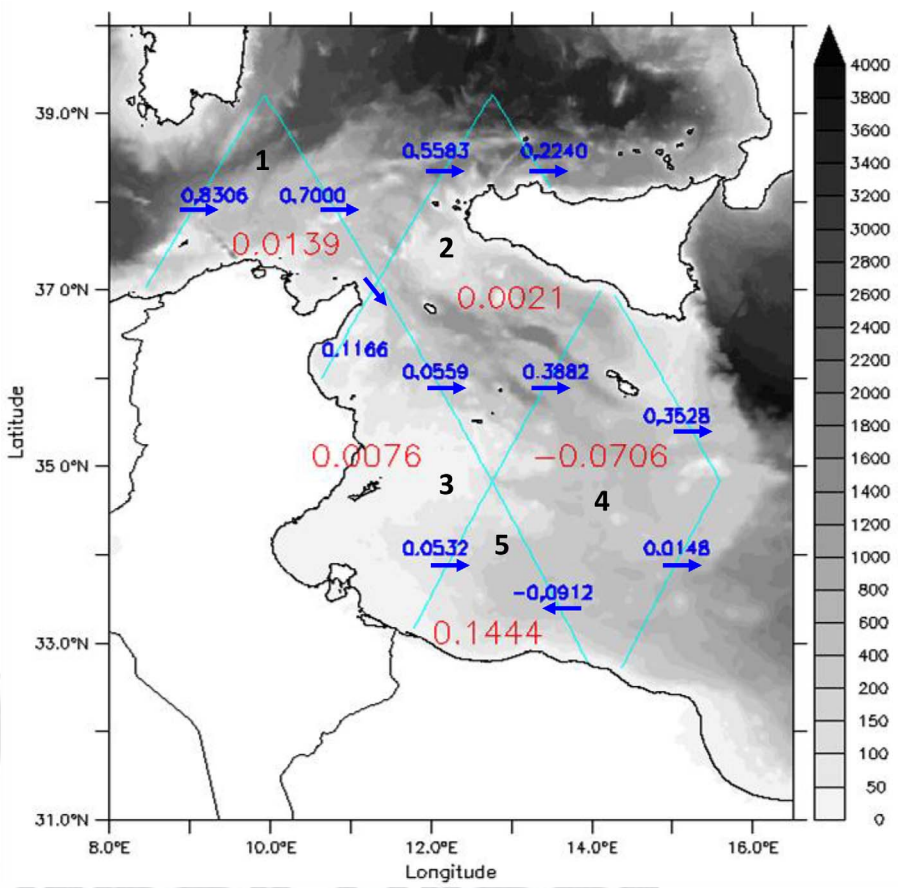

Figure 8. Mean transports (in blue) and track-closed transport residuals (in red) over the 1993–2013 period. Blue arrows indicate the orientation of the main AW transport at the boxes frontiers. Boxes number are in black and the transports unit is in Sv.

that the ALC flow across the southernmost part of track 222, in continuity with the 0.063 Sv from box 3 (track 059), is not fully resolved in the raw altimetry data set (see section 5.1 for more details).

4.4. Interannual Variations of Baroclinic Transports

The low-pass (12 months) altimeter-derived baroclinic transport time series are shown in Figure 9 for each track-closed box. Error bars in Figure 9 show the estimated error in the altimeter transports defined as ±1 standard deviation of each time series. The colors of each time series correspond to those of the tracks parts in Figure 1b. Note that the signs of the track transport estimate are set positive (negative) for inflow (outflow) and are repeated for the adjacent boxes parts. The transports through box 1 (Sardinia Channel), dominated by the AC flows, show significant interannual variability ranging from 0.6 to 1.15 Sv on track 161 and from 0.4 to 1 Sv on track 222, sometimes perfectly phased (e.g., during 1995–1996 and 2010–2011). The remaining outgoing transport from box 1 on track 237 is of minor importance (0.12 Sv on average), but has a clear increasing trend. The associated transport is also marked by several bursts in 1998, 2003, and from 2009 to 2013 with values of about ∼0.2–0.25 Sv (better depicted with the reduced range of box 3 plot in Figure 9). Though they are of the same order of magnitude as the monthly low-pass filtered box errors, they clearly follow the variability of the AW flow across track 161. F9

The incoming flows to box 2 (south and northwest of Sicily) across track 237 range from 0.2 to 0.9 Sv with a variability similar to that across tracks 161 and 222 of box 1. The 20% weakening of the AW transport between tracks 222 and 237 is likely due to some recirculation of the AW flow in the Central Mediterranean through the South Eastern Sardinia Gyre (e.g., Sorgente et al., 2011). The outgoing transport across the northern part of track 044, that would stand for the BTC, has an increasing trend with a clear regime change from positive/negative to constantly negative (i.e., eastward) flow and a lower frequency from 2 to 3–4 years

ID: kannanb Time: 13:11 I Path: //chenas03/Cenpro/ApplicationFiles/Journals/Wiley/JGRC/Vol00000/170402/Comp/APPFile/JW-JGRC170402

J_ID: JGRC Customer A_ID: JGRC22508 Cadmus Art: JGRC22508 Ed. Ref. No.: 2017JC012836 Date: 12-October-17 Stage: Page: 16

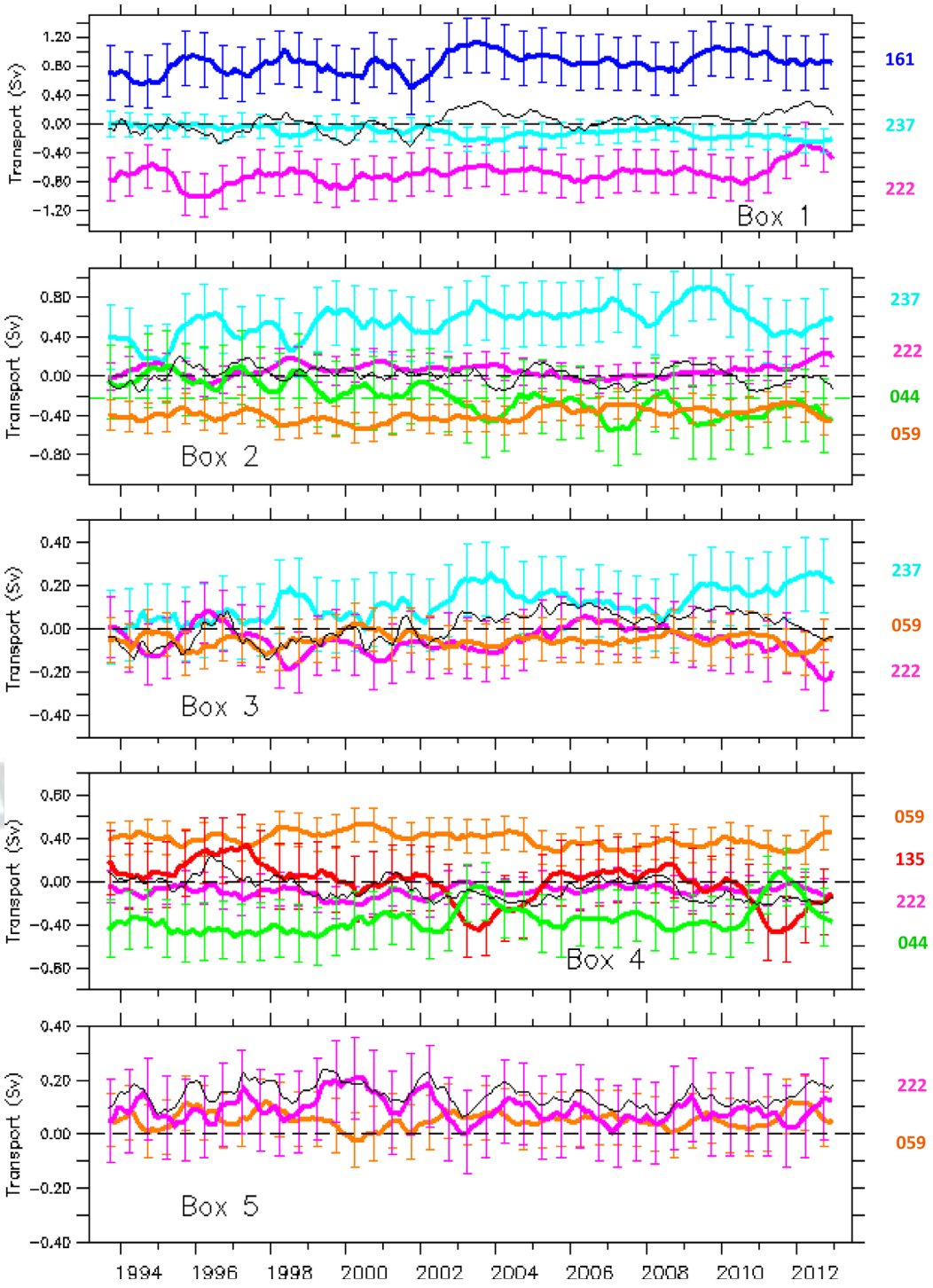

Figure 9. Time series of interannual surface transports for each of the five track-closed-boxes from 1993 to 2013. Each line color stands for a part of a track as indicated on the right of each panel and similarly to the color code of Figure 1b. The black lines are the interannual transport residuals of the track-closed-boxes. The error bars plotted every 12 months indicate the estimated error in the altimeter transport defined as ±1 standard deviation of each time series

after 1999. We believe the variations before 1999 are due to the interaction of the BTC with the Westward Northern Sicilian Current (Sorgente et al., 2011), whose signature in Figure 3 (track 044) would be the westward coastal AGVs that weaken afterward due to the increased BTC flow.

ID: kannanb Time: 13:11 I Path: //chenas03/Cenpro/ApplicationFiles/Journals/Wiley/JGRC/Vol00000/170402/Comp/APPFile/JW-JGRC170402

J_ID: JGRC Customer A_ID: JGRC22508 Cadmus Art: JGRC22508 Ed. Ref. No.: 2017JC012836 Date: 12-October-17 Stage: Page: 17

The AW transport across track 222 (middle part) is rather eastward on average when flowing from box 3 to box 2 (0.0659 Sv), but with significant fluctuations (±0.14 Sv). It shows transport increase phases during 1995, 1998, 2000–2001, and 2012 and reverse periods in 1996 and 2006 (better seen with the reduced range of box 3 plot). The outgoing flow from box 2 on track 059 does not vary much with values around 0.27–0.53 Sv all along the years. Note that after 2004, the transport time series of tracks 059 and northern 044 feature significant equivalent flows with almost the exact same amount starting from 2010. Their outflows, in antiphase with track 237 inflow, contribute in a perfectly balanced residual (Figure 9, black line, box 2). This suggests that a significant part of the increasing AW transport upstream led to an increased outflow toward the Tyrrhenian Sea, i.e., through the BTC.

The transport budget of box 3 (Gulfs of Hammamet and Gabes) relies on the northern ATC inflow on track 237 (0–0.25 Sv), the fluctuating flow across track 222 (middle part) (−0.19 to 0.08 Sv) and the constantly southern outgoing flow across the southern part of track 059 (0 to −0.15 Sv). The residual is rather negative (excess of outflow) before 2002 (except for 1996) and positive (excess of inflow) until 2012. The variability of tracks 222 and 237 derived transports is sometimes in phase, mainly during 1996 and 2006 with increased AW flows, but more frequently in antiphase i.e., compensating flows in 1994, 1998, 2000–2001, and 2012. The flow across track 059 is almost always directed eastward, which enhance the hypothesis of a significant part of the ATC flowing on the shelf toward the Gulf of Gabes (see Jebri et al., 2016). Its variability is not clearly phased with neither of the two other flows (across tracks 222 or 237).

Box 4 (southeastern shelf of Sicily and Libyan coasts) exhibits the most evident variations and has an interesting location since it is crossed by four surface features: the AIS and ATC/BATC Atlantic waters related flows from the Sicily and Tunisian shelves, respectively, the ALC on track 222 and expected interactions with the SG on track 135. The interannual variations on tracks 059 (with both the AIS and BATC flows) and 044 (mainly the AIS flow) are in good balance with quasi-equivalent transports around 0.35–0.40 Sv all over the years, except for 2003 and 2011 when the AIS related transport shows marked decreases of about 0.25 Sv. Those are clearly compensated by the marked increases of the southern outgoing transport on track 135, that may stand for a stronger BATC interacting with the SG eastward return flow as also suggested by the analysis of the interannual AGVs (see section 3). These two events of joint and opposite transport variability across tracks 044 and 135 strengthen the premise for a specular mode of the AW transport through the SC.

Box 5 holds the least significant variations, with the two transports across tracks 135 and 222 being systematically convergent (i.e., both represent inflows into the track-closed box), leading to large residuals of the transport budget. Those are more systematically associated with track 222 transport estimates, with a 1–3 years variability. Note that the same apparent covariability is observed on the residuals of box 4, suggesting a critical deficiency of the transport-like model regarding the southern part of track 222 as also discussed above in section 4.3.

5. Discussion

5.1. Limitations of the Proxy Method for Transport Estimation

Our transport-like approach allowed to better quantify the different AW related flows while taking into account the strong bathymetry constraints of the SC. This transport-like approach appears globally efficient, as the long-term averaged transport budgets gave low residuals, at least for the boxes over the deepest areas, and mean transports are in the range of previous estimates for the AC flow (0.5–1.5 Sv) at the entrance or inside the SC (e.g., Astraldi et al., 1996; Buongiorno Nardelli et al., 2006; Onken et al., 2003; Sammari et al., 1995). Budget uncertainties for boxes 3 and 5 over shallow areas, however, show the limits of such altimetry-derived approach, requiring thus to be discussed in-depth.

First, although the altimetry product used here is posttreated for coastal zone applications, errors of SLA estimates at endpoints could be crucial for narrow coastal jet, especially the ALC that is thought to be insufficiently resolved for a balanced transport budget in boxes 4 and 5. The Tunisian-Libyan shelf area shows a drastic reduction of the continental shelf where tidal resonance with amplitudes of 2 m may occurs (e.g., Sammari et al., 2006), so that one may question the ability of the regional MOG2D tidal model used in the X-TRACK data treatment to remove such strong tidal harmonic in this specific area. Second, the prevalence of the SG current patterns over track 135 derived AGV questions the strong assumption of a homogeneous

ID: kannanb Time: 13:11 I Path: //chenas03/Cenpro/ApplicationFiles/Journals/Wiley/JGRC/Vol00000/170402/Comp/APPFile/JW-JGRC170402

AGU Journal of Geophysical Research: Oceans 10.1002/2017JC012836

baroclinic model for the whole area. Though previous work suggested that the SG could possibly modulate the seasonal AW outflow outside the SC (Ciappa, 2009; Gerin et al., 2009; Jebri et al., 2016; Poulain & Zambianchi, 2007; Sorgente et al., 2011), there is no reason for its vertical structure to be similar to the AW related geostrophic currents, such as the ATC and AIS. This also questions the hypothesis of a constant baroclinicity for all tracks, as significant variations of the AW/LIW interface depth in the center of the SC was observed from hydrographic data at different time scales ranging from weeks to seasons and even up to multiyear (e.g., Ben Ismail et al., 2012, 2014; Sammari et al., 1995).

Other factors such as the aliasing of high-frequency (<1 month) mesoscale patterns in the monthly means may also lead to flow and transport-like uncertainties. Sorgente et al. (2003) found from numerical modeling a transport baroclinic component ranging from 1.0 to 1.8 Sv. Onken et al. (2003) estimated an eastward AW transport entering the Sicily Channel of ∼1.3 Sv with a barotropic contribution of 0.4 Sv for October 1996. This gives a 0.9 Sv estimate for the baroclinic transport of AW inflowing the SC, close to the value computed here for tracks 161 and 222 (0.7–0.8 Sv on average, ∼1 Sv in Figure 9 for 1996) and only slightly higher than the monthly estimate of 0.8 Sv computed from tracks 237 and 044 for the same period. This estimate is reduced to 0.56 Sv with the 12 months low-pass filter in Figure 9, but Figure 7 shows that monthly estimates rather varies over the range of previous estimates. On the other hand, a mean baroclinic AW transport of 0.49 Sv is given in Korres et al. (2000) through the SC, while the few estimates of Buongiorno Nardelli et al. (2006) varies from 0.43 to 1.43 Sv for a 0–300 dbar vertical section over the deepest part of track 059. Likewise, the northern inflow of track 237 (ATC) shows values during 2003 in agreement with the transport estimate of Ben Ismail et al. (2012) from in situ geostrophic and adjusted currents over the 0–150 m layer.

The 10 days time return of the initial TOPEX and Jason1–2 data for a track limits the ability of the altimetry data to fully capture the strong mesoscale activity associated with the numerous narrow currents, fronts and eddies as well as their possible interactions. Poorly resolved mesoscale variability between tracks at short time scales (5–10 days) may be aliased in monthly means and lead to significant errors in the transport-like estimates and track-closed box budgets. Nevertheless, the variances of the residuals are always significantly lower than the sum of the variances of the corresponding transports (see Table 4), suggesting that if some deviations from the model assumptions can lead to significant monthly transport budget errors, these errors nearly compensate each other on longer time scales. Moreover, the low-frequency modulation of the mesoscale variability may generate long-term anomalies in the surface circulation patterns or in the water masses and, consequently, explain a significant part of the interannual variability of the AW flow (Fernandez et al., 2005; Larnicol et al., 2002). Some elements to support our results may be found in the 11 years study of eddy kinetic energy from altimetric data of Pujol and Larnicol (2005), such as a significant increase of the EKE along the BATC path in 2003 for a preferential southern AW outflow mode discussed above and over the Sicily upwelling area in 1999 and 2001, in support to the offshore migration of the AIS flow in Figure 3.

Lastly, the 12 months low-pass filter monthly residuals seem likely nonsignificant in boxes 1, 2, and even 4, hence over the deepest areas which exhibit major (>0.4 Sv) inflows and outflows. They may seem more questionable in box 3, which is on the Tunisian shelf and where the strong bathymetry constraint on the flow may increase the errors, whether through the tidal model corrections or baroclinic deviation from the transport-like model. The near along-slope orientation of track 222, crossing the main ATC path, with a

Table 4
Average Statistics of Surface Transport Over Track-Closed-Boxes

Box Number	Mean (AWT)	Variance (AWT)	∑ (Variance (AWT))
1	0.0139 Sv	0.1515 Sv^2	0.2577 Sv^2
2	0.0021 Sv	0.0921 Sv^2	0.2865 Sv^2
3	0.0076 Sv	0.0399 Sv^2	0.0581 Sv^2
4	−0.0706 Sv	0.0971 Sv^2	0.2103 Sv^2
5	0.1444 Sv	0.0274 Sv^2	0.0334 Sv^2

Note. AWT stands for Atlantic Water Transport. The third column stands for the sum of the transport variances of each track-closed-box side.

J_ID: JGRC Customer A_ID: JGRC22508 Cadmus Art: JGRC22508 Ed. Ref. No.: 2017JC012836 Date: 12-October-17 Stage: Page: 19

bathymetry ranging between 40 and 390 m, is likely the main source of such uncertainties, as yet suggested for boxes 3 and 5 in section 4.1. Nevertheless, we rely on the good transport budget for the deepest track-closed boxes, especially the conservation of the mean AW baroclinic flow of 0.4 Sv all over the SC, even with the significant part (0.12 Sv) transiting through the Tunisian shelf. We, therefore, assume that our analysis helps to quantify some major year-to-year changes in the pathways of AW transport throughout the studied area.

5.2. Main Interannual Variability Modes of the AW Circulation in the SC

Over the 20 year time series of altimetry surface current and associated transports, we first notice a significant trend for an increased inflow of AW in the Tunisia-Sicily-Sardinia area with a marked interannual variability that is unequally shared between the ATC and AIS inflows in the SC and the BTC outflow northeast of Sicily. The surface ATC related currents near Cape Bon, and potentially the associated transport from box 1 to 3, reaches the strongest intensities during 1998, 2003, 2009, and 2012, always associated with increased AW flows through track 161. These AW pulses are also seen on the upper part of track 237 as an inflow to box 2, but are often compensated by an increased BTC outflow across the upper part of track 044. This led to a nearly constant southeast AW flow throughout boxes 2 and 4, while the regime shift in the BTC surface current and transports over the upper part of track 044 clearly follows the long-term tendency of an increased AW flow. This suggest that the interannual and long-term variability of the external upcoming AW flow would be primarily distributed through the ATC and BTC flows, the AIS related one being less variable.

The low variability of the AIS related AW transports for both tracks 059 and 044 (see Figure 9) may appear somewhat surprising given the marked variability of surface velocities across track 059 (Figure 3), that show wide expansions offshore during 1994–1996, 2005–2006, and 2009–2010. The high variability of the AIS flow off Sicily is a well-known feature due to the interaction with the Sicily upwelling driven by a joint effect of wind stress and bathymetry constraints over the Adventure Bank (e.g., Bonanno et al., 2014; Grancini & Michelato, 1987; Piccioni et al., 1988). Béranger et al. (2004) and Jouini et al. (2016) argue that this upwelling may be also reinforced by the westward advection of Ionian waters at depth through Kelvin-like trapped coastal waves along the Sicilian coast. By contrast, both the surface AGVs (Figure 3) and transport estimates (Figure 9) across track 044 in the SC are significantly less variable, showing only two marked decreases in 2003 and 2011. Note that the northern part of track 059 (box 2 boundary) include both the ATC/BATC and AIS flows and that the high mesoscale variability in the central part of the SC may lead to recirculation patterns between them. The crossing between tracks 222 and 237 near Cape Bon, being in the middle of the main ATC vein of currents, prevents us from clearly quantifying the relative contribution of the AW flowing over the Tunisian shelf with regard to the one along-slope. Several eastward pulses across track 222 are associated with the AW inflow pulses in support to a rapid recirculation toward the central part of the SC in 1994–1995, 1998, 2000–2001, and 2012. In addition, the fluctuating westward AVG between 35.5°N and 36.2°N on both tracks 059 and 044 (Figure 3) would sign such possible recirculation patterns and may explain the low variability of the AIS related transport over the 20 year time series.

The last major pattern highlighted in our analysis is the shift in the preferential AW outflow to the Eastern Mediterranean from track 044 (northern SC) to track 135 (southern SC) in 2003 and 2011, suggesting interactions with the southward SG. Those are signed on both the AVG and transport estimates, each being associated with an increased BATC flow upstream (tracks 222 and 059). Nevertheless, only the first one seems to be driven by an increased AW flow from the AC (tracks 161, Figures 3 and 9) and ATC (track 237, Figures 3 and 9 for box 3). A similar BATC/SG coupling is detectable in 1999–2000, but with no effect on the mean AW outflow, as well as an intensification of the SG in 1998–1999. This interannual variability mode of the AW flow over the SC is identified in Jouini et al. (2016) from a neural cluster analysis of a 46 years Mediterranean circulation simulation (NEMO 1/12°). Their analyses revealed a very significant signal for this circulation mode during summer 1999, 2003, and 2011, consistent with our findings. To better support this assumption, we illustrate in Figure 10 typical summer situations where the AW would rather exit the SC primarily through the BATC (summers of 2003 and 2011), or on the contrary by the dominant AIS flow (summer of 2005 and the 20 years summer climatology). It clearly shows the prominence of the ATC/BATC surface geostrophic velocity in 2003 and 2011 over the AIS related ones. The summer 2005 and climatological situations show an AIS flow associated with a marked tongue of colder AW that propagates northward in the Ionian Sea along the East coast of Sicily. The thermal signature of the BATC flow toward the southern

ID: kannanb Time: 13:11 I Path: //chenas03/Cenpro/ApplicationFiles/Journals/Wiley/JGRC/Vol00000/170402/Comp/APPFile/JW-JGRC170402

AGU Journal of Geophysical Research: Oceans 10.1002/2017JC012836

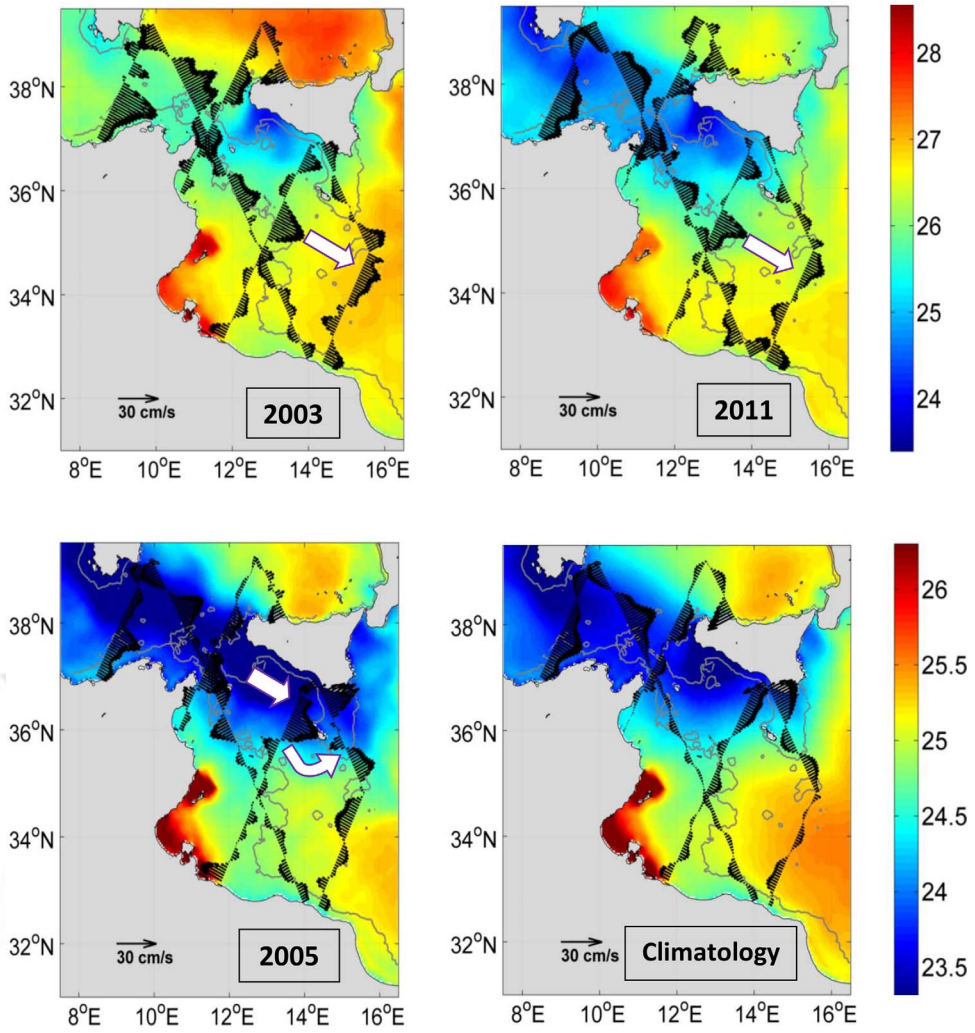

Figure 10. Summer (June–July–August) mean of cross-track currents and SST maps for 2003, 2005, and 2011. The summer season climatology is also shown. The 200 m isobath (grey solid line) is from ETOPO2v1 global gridded database. The white arrows show the preferential path of that Atlantic Waters follow to exit the Sicily Channel.

Ionian Sea is more marked in 2011 than in 2003 likely due to the overall heating of the surface layer during the 2003 heat wave on the Central Mediterranean Sea (e.g., Olita et al., 2007). They attributes the summer 2003 AIS weakening to a decreased longitudinal density gradient over the SC, due to the heat wave induced heating over the area, and reduced wind forcing of the Sicilian upwelling, with a compensating increased BATC. The turbulent AW flow toward the Tunisian shelf is signed in all cases by a tongue of slightly colder surface temperature, interleaved between the warm coastal waters of the Gulf of Gabes and those from the southern Ionian Sea. This thermal signature of the AW flow over the shelf is less pronounced in 2003 and 2011, with reference to the two other situations, likely due to increased mesoscale variability over the Tunisian-Libyan shelf and the possible flow interactions with the SG. Lastly, the more evident signature of the ALC flow in the southeastern part of the shelf during 2003 and 2011 supports an increased AW flow toward the southern Ionian Sea.

5.3. Possible Connection between Transport Variations and External Factors

In this subsection, we discuss the large-scale oceanographic and atmospheric factors that may cause the interannual variations of the surface currents and transports over the SC. One of those, is the Ionian Bimodal Oscillating System (BiOS) dynamics (Gačić et al., 2013, 2014). The BiOS anticyclonic mode intensifies the spreading of the AW into the northern Ionian while the cyclonic situation implies a wider spreading of AW in the southeastern basin (Bonanno et al., 2014). Knowing that tracks 044 and 135 catches a part of the

J_ID: JGRC Customer A_ID: JGRC22508 Cadmus Art: JGRC22508 Ed. Ref. No.: 2017JC012836 Date: 12-October-17 Stage: Page: 21

Ionian circulation, the particular events of the BATC and SG around 33.2°N–34.2°N in 1997–1998 in Figure 3 (track 044 + 135) and the two BATC events of 2003 and 2011 (see Cardin et al., 2015; Gačić et al., 2014) are possibly related to the BiOS variability. Part of the interannual variability could also be linked to the Eastern Mediterranean Transient (EMT) that may act through water masses modifications in the Sicily Channel (Gasparini et al., 2005; Roether et al., 2007), to the North Atlantic Oscillation (NAO) likely affecting the global Mediterranean circulation (Rixen et al., 2005; Vignudelli et al., 1999) or even the local winds. Cardin et al. (2015) argue that the relaxation phase of the EMT lasted for the last 20 years, while Gasparini et al. (2005) suggest that a further EMT evolution can be diagnosed after 1999 at the entry of the SC with a decrease (increase) of AW (LIW) salinity of similar magnitude as in 1992–1993. The resulting salinity horizontal variations and density gradients would then induce intense surface currents (by geostrophy) and the eastern basin would be reached by fresher surface water during a higher EMT like phase (Gasparini et al., 2005). How this long-term relaxation of the main 1992–1993 EMT event lies with the long-term tendency of increased AW flow toward the SC, suggested by our analysis, is unclear, but this does not exclude the possibility of pulsed outflow of modified LIW affecting the AW flow surface signature. Except the AW flow in the Sardinia channel and the ALC sudden increase at midterm of the 20 year time series, there is no obvious variability on the main AW flow paths that would be consistent with a NAO-like decadal time scale. Moreover, the connection between the NAO and the Mediterranean circulation is not fully understood, being possibly different among subregions (e.g., Rixen et al., 2005) or interacting with the BiOS (e.g., Pinardi et al., 2016) or the EMT (e.g., Tsimplis & Josey, 2001).

Although regional AW structures in the SC are mainly driven by large-scale thermohaline circulation, the winds may have a significant role. The geostrophic component of the circulation is not directly influenced by the local winds, but rather indirectly via the baroclinic instabilities (Omrani et al., 2016). As such, the intense north-west summer winds contribute in the generation of the upwelling off Sicily and influence the variability of the AIS flow (Sorgente et al., 2011). Other studies (e.g., Poulain & Zambianchi, 2007) showed similar results with a correspondence between the AIS and ATC and Mistral-like wind regimes, while low currents were rather associated with weaker southerly winds. In terms of transports, Béranger et al. (2005) estimated a relatively low correlation of 0.3 between the intensity of local wind and the eastward transport through the SC. Here, we estimate an order of magnitude of the Ekman transport over the study area following Pickett and Paduan (2003):

$$TE = \frac{\tau}{\rho w\ f} \tag{4}$$

where τ is the along-transect component of surface wind stress, ρ_w is the density of seawater (assumed constant at 1024 kg m^{-3}), and f is the Coriolis parameter. The quadratic stress law of Large and Pond (1981) was used to obtain wind stress from wind velocity:

$$\tau = \rho \mathrm{aCd} U\mathrm{wind2} \tag{5}$$

where ρ_a ($\sim$1.225 kg m^{-3}) is the air density and the dimensionless friction coefficient C_d is taken as 0.0013 for U_{wind} <11 m s^{-1} (Large & Pond, 1981) as it is the case for the Sicily Channel. According to the model of Omrani et al. (2016) relevant surface winds in the region were typically from the northwest at 6–10 m s^{-1}. Following equation (5), these winds would produce near shore wind stresses of approximately 0.037 N m^{-2} (for latitudes around 37°N), which, in turn, would yield offshore Ekman transports of 0.008 Sv. This transport associated to the Ekman effect is very small (more than two orders of magnitude) compared to the geostrophic component computed above and can be neglected. More, it is a high-frequency signal which, thus, would not affect our budget on the low frequency, i.e., from the seasonal to the interannual time scale (Han & Tang, 2001). Anyhow, our knowledge about the contribution of local changes in winds in the interannual current and transport variations over the SC is yet to be refined.

6. Summary and Perspectives

This study conducts a specific analysis of the surface geostrophic currents through the Sicily Channel as derived from along-track absolute dynamic topography over a 20 years data set. This allows monitoring of the interannual fluctuations of several boundary currents, i.e., the AC, ATC, AIS, BATC, ALC, and SG that spread the Atlantic Waters over this study area. Our analysis also reveals a spatial track-to-track coherency

ID: kannanb Time: 13:11 I Path: //chenas03/Cenpro/ApplicationFiles/Journals/Wiley/JGRC/Vol00000/170402/Comp/APPFile/JW-JGRC170402

AGU Journal of Geophysical Research: Oceans 10.1002/2017JC012836

observed consistently over the entire length of the altimetry period, despite the marked interannual variability (Figures 3 and 7). We estimate the associated AW baroclinic transport via a transport-like model that, despite the caveats, agrees relatively well with historical observations and/or numeric modeling. The model finds two significant modes of variability, (1) a long-term tendency for an increased AW flow benefiting preferentially to the BTC and the ATC/ALC systems, and (2) a shift AW flow from the AIS, as the predominant mode, to the BATC and SG systems for 2 years over the 20 year time series. Furthermore, the analysis gives better insights on the variability of the transport flow over the wild shelf of Tunisia.

In a context of scarce hydrographic measurements and the difficulty and cost of maintaining dense in situ network, our study proves that coastal altimetry can be a highly useful tool for obtaining long time series of the water transport over the whole SC region and with a relatively good spatial resolution. Furthermore, the upcoming altimetry missions (e.g., the CNES/ISRO SARAL-AltiKa Mission in Ka-band, the ESA CryoSat-2 and COPERNICUS Sentinel-3, Sentinel-6 Mission in SAR mode) will significantly reduce measurement noise and increase the along-track resolution. This would help improve the observations over the more coastal areas, especially the Tunisian-Libyan shelf where our approach seemed deficient. The use of these new coastal altimetry observations, in the expectation of the improvements of satellite Sea Surface Salinity over enclosed Seas such as the Mediterranean, in synergy with other data sources and modeling tools will enable a better understanding of the structure and evolution of the currents in the Central Mediterranean. Particularly, the recent availability of suitable ocean circulation reanalysis (e.g., Hamon et al., 2016; Pinardi et al., 2016) would help answer the main remaining open questions about the relative strength of internal (e.g., regional atmospheric forcing and mesoscale activity) and external (e.g., atmospheric and climatologic effects) factors that would explain the long-term tendency and particular events revealed by our analysis.

Acknowledgments
This work is part of the PhD of Madame Jebri Fatma. This publication was produced with the financial support of the Allocations de recherche pour une thèse au sud (ARTS) program of the Institut de Recherche pour le Développement (IRD). The X-TRACK altimetry data used in this study were developed, validated, and distributed by the CTOH/LEGOS, France (http://ctoh.legos.obs-mip.fr/products/coastal-products/coastal-products-1/sla-1hz/medsea/). The processed and validated hydrographic data were provided through SeaDataNet Pan-European infrastructure for ocean and marine data management (http://www.seadatanet.org), the SST ones by the Copernicus Marine Environment Monitoring Service (http://marine.copernicus.eu/).

References

Astraldi, M., Baloupoulos, S., Candela, J., Font, J., Gacic, M., Gasparini, G. P., . . . Tintoré, J. (1999). The role of straits and channel in understanding the characteristics of Mediterranean circulation. *Progress in Oceanography*, *44*, 64–108. https://doi.org/10.1016/S0079-6611(99)00021-X

Astraldi, M., Gasparini, G. P., Sparnocchia, S., Moretti, M., & Sansone, E. (1996). The characteristics of the water masses and the water transport in the Sicily Strait at long time scales, In F. Briand (Ed.), *Dynamics of Mediterranean straits and channels* (Vol. 17, pp. 95–115). Bulletin de l'Institut Oceanographique. Retrieved from http://ciesm.org/online/monographs/CSS-2/CSS_2_95_115.pdf

Ben Ismail, S., Sammari, C., Gasparini, G. P., Béranger, K., Brahim, M., & Aleya, L. (2012). Water masses exchanged through the Sicily Channel: Evidence for the presence of new water masses on Tunisian side of the Channel. *Deep Sea Research Part I: Oceanographic Research Papers*, *63*, 65–81. http://doi.org/10.1016/j.dsr.2011.12.009

Ben Ismail, S., Schroeder, K., Sammari, C., Gasparini, G. P., Borghini, M., & Aleya, L. (2014). Inter-annual variability of water mass properties in the Tunisia-Sicily Channel. *Journal of Marine Systems*, *135*, 14–28. http://doi.org/10.1016/j.jmarsys.2013.06.010

Benzohra, M., & Millot, C. (1995). Characteristics and circulation of the surface and intermediate water masses off Algeria. *Deep Sea Research Part I: Oceanographic Research Papers*, *42*(10), 1803–1830. https://doi.org/10.1016/0967-0637(95)00043-6

Béranger, K., Mortier, L., & Crépon, M. (2005). Seasonal variability of water transports through the Straits of Gibraltar, Sicily and Corsica, derived from a high resolution model of the Mediterranean circulation. *Progress in Oceanography*, *66*(2–4), 341–364. https://doi.org/10.1016/j.pocean.2004.07.013

Béranger, K., Mortier, L., Gasparini, G. P., Gervasio, L., Astraldi, M., & Crepon, M. (2004). The dynamics of the Sicily strait: A comprehensive study from observations and models. *Deep Sea Research Part II: Topical Studies in Oceanography*, *51*(4–5), 411–440. https://doi.org/10.1016/j.dsr2.2003.08.004

Birol, F., Cancet, M., & Estournel, C. (2010). Aspects of the seasonal variability of the Northern Current (NW Mediterranean Sea) observed by altimetry. *Journal of Marine Systems*, *81*(4), 297–311. https://doi.org/10.1016/j.jmarsys.2010.01.005

Bonanno, A., Placenti, F., Basilone, G., Mifsud, R., Genovese, S., Patti, B., . . . Mazzola, S. (2014). Variability of water mass properties in the Strait of Sicily in summer period of 1998–2013. *Ocean Science*, *11*, 811–837. https://doi.org/10.5194/os-10-759-2014

Borzelli, G., & Ligi, R. (1998). Autocorrelation scales of the SST distribution and water masses stratification in the channel of Sicily. *Journal of Atmospheric Oceanic Technology*, *16*, 776–782. https://doi.org/10.1175/1520-0426(1999)016<0776:ASOTSD>2.0.CO;2

Bosse, A., Testor, P., Mortier, L., Prieur, L., Taillandier, V., D'ortenzio, F., & Coppola, L. (2015). Spreading of Levantine Intermediate Waters by submesoscale coherent vortices in the northwestern Mediterranean Sea as observed with gliders. *Journal of Geophysical Research: Oceans*, *120*, 1599–1622. https://doi.org/10.1002/2014JC010263

Bouffard, J. (2007, November). Amélioration de l'altimétrie côtière appliquée à l'étude de la circulation dans la partie nord du bassin occidental Méditerranéen (Thèse de Doctorat) de l'Université Toulouse III.

Bouffard, J., Pascual, A., Ruiz, S., Faugère, Y., & Tintoré, J. (2010). Coastal and mesoscale dynamics characterization using altimetry and gliders: A case study in the Balearic, Sea. *Journal of Geophysical Research*, *115*, C10029. https://doi.org/10.1029/2009JC006087

Bouffard, J., Roblou, L., Birol, F., Pascual, A., Feneglio-Marc, L., Cancet, M., . . . Menard, Y. (2011). Introduction and assessment of improved coastal altimetry strategies: Case study over the North Western Mediterranean Sea. In S. Vignudelli, A. Kostianoy, P. Cipollini, & J. Benveniste (Eds.), *Coastal altimetry* (Chapter 12, pp. 297–330). Berlin, Germany: Springer. https://doi.org/10.1007/978-3-642-12796-0_12

Bouffard, J., Vignudelli, S., Cipollini, P., & Menard, Y. (2008). Exploiting the potential of an improved multimission altimetric data set over the coastal ocean. *Geophysical Research Letters*, *35*, L10601. https://doi.org/10.1029/2008GL033488

Buongiorno Nardelli, B., Cavalieri, O., Rio, M.-H., & Santoleri, R. (2006). Subsurface geostrophic velocities inference from altimeter data: Application to the Sicily Channel (Mediterranean Sea). *Journal of Geophysical Research*, *111*, C04007. https://doi.org/10.1029/2005JC003191

J_ID: JGRC Customer A_ID: JGRC22508 Cadmus Art: JGRC22508 Ed. Ref. No.: 2017JC012836 Date: 12-October-17 Stage: Page: 23

Buongiorno Nardelli, B., Santoleri, R., Zoffoli, S., & Marullo, S. (1999). Altimetric signal and three-dimensional structure of the sea in the Channel of Sicily. *Journal of Geophysical. Research*, *104*(C9), 585–603. https://doi.org/10.1029/1999JC900103

Buongiorno Nardelli, B., Sparnocchia, S., & Santoleri, R. (2001). Small mesoscale features at a meandering upper ocean front in the western Ionian Sea (Mediterranean Sea): Vertical motion and potential vorticity analysis. *Journal of Physical Oceanography*, *31*(8), 2227–2250. https://doi.org/10.1175/1520-0485(2001)031<2227:SMFAAM>2.0.CO;2

Buongiorno Nardelli, B., Tronconi, C., Pisano, A., & Santoleri, R. (2013). High and Ultra-high resolution processing of satellite Sea Surface Temperature data over Southern European Seas in the framework of MyOcean project. *Remote Sensing of Environment*, *129*, 1–16. https://doi.org/10.1016/j.rse.2012.10.012

Cardin, V., Civitarese, G., Hainbucher, D., Bensi, M., & Rubino, A. (2015). Thermohaline 17 properties in the Eastern Mediterranean in the last three decades: Is the basin returning to the 18 pre-EMT situation? *Ocean Science*, *11*, 53–66. http://doi.org/10.5194/os-11-53-2015

Casey, K. S., Brandon, T. B., Cornillon, P., & Evans, R. (2010). The past, present and future of the AVHRR pathfinder SST program. In V. Barale, J. F. R. Gower, & L. Alberotanza (Eds.), *Oceanography from space* (Chapter 16, pp. 273–287). Dordrecht, the Netherlands: Springer. http://doi.org/10.1007/978-90-481-8681-5_16

Ciappa, A. C. (2009). Surface circulation patterns in the Sicily Channel and Ionian Sea as revealed by MODIS chlorophyll images from 2003 to 2007. *Continental Shelf Research*, *29*(17), 2099–2109. http://doi.org/10.1016/j.csr.2009.08.002

Deng, X., Hwang, C., Coleman, R., & Featherstone, W. E. (2008). Seasonal and inter-annual variations of the Leeuwin Current off Western Australia from TOPEX/Poseidon Satellite Altimetry. *Terrestrial, Atmospheric and and Ocean Sciences*, *19*(1–2), 135–149. https://doi.org/10.3319/TAO.2008.19.1-2.135(SA)

Fernandez, V., Dietrich, D. E., Haney, R. L., & Tintoré, R. L. (2005). Mesoscale, seasonal and inter-annual variability in the Mediterranean Sea using a numerical ocean model. *Progress in Oceanography*, *66*(2–4), 321–340. https://doi.org/10.1016/j.pocean.2004.07.010

Fofonoff, N. P. (1962). Dynamics of ocean currents. In M. N. Hill (Ed.), *The sea. Vol. 1: Physical oceanography* (pp. 323–395). New York, NY: Wiley-Interscience.

Gačić, M., Civitarese, G., Kovačević, V., Ursella, L., Bensi, M., Menna, M., . . . Pizzi, C. (2014). Extreme winter 2012 in the adriatic: An example of climatic effect on the Biosrhythm. *Ocean Science*, *10*, 513–522. https://doi.org/10.5194/os-10-513-2014

Gačić, M., Schroeder, K., Civitarese, G., Cosoli, S., Vetrano, A., & Eusebi Borzelli, G. L. (2013). Salinity in the Sicily Channel corroborates the role of the Adriatic-Ionian Bimodal Oscillating System (BiOS) in shaping the decadal variability of the Mediterranean overturning circulation. *Ocean Science*, *9*, 83–90. https://doi.org/10.5194/os-9-83-2013

Garzoli, S., & Maillard, C. (1979). Winter circulation in the Sicily and Sardinia Straits region. *Deep Sea Research Part A: Oceanographic Research Papers*, *26*(8), 933–954. https://doi.org/10.1016/0198-0149(79)90106-7

Gasparini, G. P., Ortona, A., Budillon, G., Astraldi, M., & Sansone, E. (2005). The effect of the Eastern Mediterranean Transient on the hydrographic characteristics in the Strait of Sicily and in the Tyrrhenian Sea. *Deep Sea Research Part I: Oceanographic Research Papers*, *52*, 915–935. https://doi.org/10.1016/j.dsr.2005.01.001

Gasparini, G. P., Schroder, K., Vetrano, A., & Astraldi, M. (2007). Canali e stretti quali punti di osservazione privilegiata per lo studio della variabilita inter-annuale del bacino Mediterraneo. In CNR–Roma (Ed.), *Clima e cambiamenti climatici: le attivita di ricerca del CNR* (pp. 521–524). Retrieved from http://www.irpi.to.cnr.it/documenti/CNR_Volume_Clima.pdf. AQ11

Gasparini, G. P., Smeed, D. A., Alderson, S., Sparnocchia, S., Vetrano, A., & Mazzola, S. (2004). Tidal and subtidal currents in the Strait of Sicily. *Journal of Geophysical Research*, *109*, C02011. https://doi.org/10.1029/2003JC002011

Gerin, R., Poulain, P. M., Taupier-Letage, I., Millot, C., Ben Ismail, S., & Sammari, C. (2009). Surface circulation in the Eastern Mediterranean using drifters (2005–2007). *Ocean Science*, *5*, 559–574. https://doi.org/10.5194/os-5-559-2009

Grancini, G. F., & Michelato, A. (1987). Current structure and variability in the Strait of Sicily and adjacent area. *Annales Geophysicae, Series B*, *5*, 75–88.

Hamon, M., Beuvier, J., Somot, S., Lellouche, J. M., Greiner, E., Jordà, G., . . . Drillet, Y. (2016). Design and validation of MEDRYS, a Mediterranean Sea reanalysis over the period 1992–2013. *Ocean Science*, *12*, 577–599. https://doi.org/10.5194/os-12-577-2016

Han, G., & Tang, C. L. (2001). Inter-annual variation of volume transport in the western Labrador Sea based on TOPEX/Poseidon and WOCE data. *Journal of Physical Oceanography*, *31*, 199–211. https://doi.org/10.1175/1520-0485(2001)031<0199:IVOVTI>2.0.CO;2

Jebri, F., Birol, F., Zakardjian, B., Bouffard, J., & Sammari, C. (2016). Exploiting coastal altimetry to improve the surface circulation scheme over the central Mediterranean Sea. *Journal of Geophysical Research: Oceans*, *121*, 4888-4909. https://doi.org/10.1002/2016JC011961

Jouini, M., Béranger, K., Arsouze, T., Beuvier, J., Thiria, S., Crépon, M., & Taupier-Letage, I. (2016). The Sicily Channel surface circulation revisited using a neural clustering analysis of a high-resolution simulation. *Journal of Geophysical Research: Oceans*, *121*, 4545–4567. https://doi.org/10.1002/2015JC011472

Korres, G., Pinardi, N., & Lascaratos, A. (2000). The ocean response to low-frequency inter-annual atmospheric variability in the Mediterranean sea: Part I. Sensitivity experiments and energy analysis. *Journal of Climate*, *13*, 705–731. https://doi.org/10.1175/1520-0442(2000)013<0705:TORTLF>2.0.CO;2

Lacombe, H., & Tchernia, P. (1972). Caractères hydrologiques et circulation des eaux en Méditerranée. In D. J. Stanley (Ed.), *The Mediterranean Sea: A natural sedimentation laboratory* (pp. 25–36). Stroudsburg, PA: Dowden Hutchinson and Ross.

Large, W. G., & Pond, S. (1981). Open ocean momentum flux measurements in moderate to strong wind stress over the world ocean with error estimates. *Journal of Physical Oceanography*, *11*, 324–336. https://doi.org/1520-0485(1981)011<0324:OOMFMI>2.0.CO;2

Larnicol, G., Ayoub, N., & Le Traon, P. Y. (2002). Major changes in Mediterranean Sea level variability from 7 years of TOPEX/Poseidon and ERS-1/2 data. *Journal of Marine Systems*, *33–34*, 63–89. https://doi.org/10.1016/S0924-7963(02)00053-2

Le Hénaff, M., Roblou, L., & Bouffard, J. (2011). Characterizing the Navidad Current inter-annual variability using coastal altimetry. *Ocean Dynamics*, *61*(4), 425–437. https://doi.org/10.1007/s10236-010-0360-9

Lermusiaux, P. F. J., & Robinson, A. R. (2001). Features of dominant mesoscale variability, circulation patterns and dynamics in the Strait of Sicily. *Deep Sea Research Part I: Oceanographic Research Papers*, *48*(9), 1953–1997. https://doi.org/10.1016/S0967-0637(00)00114-X

Malanotte-Rizzoli, P., Artale, V., Borzelli-Eusebi, G. L., Brenner, S., Crise, A., Gacic, M., . . . Triantafyllou, G. (2014). Physical forcing and physical/biochemical variability of the Mediterranean Sea: A review of unresolved issues and directions for future research. *Ocean Science*, *10*(3), 281–322. https://doi.org/10.5194/os-10-281-2014

Manzella, G. M. R. (1994). The seasonal variability of water masses and transport through the Strait of Sicily. In P. E. La Violette (Ed.), *Seasonal and inter-annual variability of the Western Mediterranean Sea* (Vol. 46, pp. 33–45). Washington, DC: American Geophysical Union. https://doi.org/10.1029/CE046p0033

Manzella, G. M. R., Gasparini, G. P., & Astraldi, M. (1988). Water exchange between eastern and western Mediterranean through the Strait of Sicily. *Deep Sea Research Part A: Oceanographic Research Papers*, *35*(6), 1021–1036. https://doi.org/10.1016/0198-0149(88)90074-X

ID: kannanb Time: 13:11 I Path: //chenas03/Cenpro/ApplicationFiles/Journals/Wiley/JGRC/Vol00000/170402/Comp/APPFile/JW-JGRC170402

AGU Journal of Geophysical Research: Oceans 10.1002/2017JC012836

Millot, C., & Taupier-Letage, I. (2005). Circulation in the Mediterranean Sea. In A. Saliot (Ed.), *The Mediterranean sea, handbook of environmental chemistry* (Vol. 5k, pp. 29–66). Berlin, Germany: Springer. https://doi.org/10.1007/b107143

Napolitano, E., Sannino, G., Artale, V., & Marullo, S. (2003). Modeling the baroclinic circulation in the area of the Sicily Channel: The role of stratification and energy diagnostics. *Journal Geophysical Research*, *108*(C7), 3230. https://doi.org/10.1029/2002JC001502

Nielsen, J. N. (1912). Hydrography of the Mediterranean and adjacent waters. In J. Schmidt (Ed), *Report of the Danish Oceanographic Expedition 1908–1910 to the Mediterranean and adjacent waters* (Vol. 1, pp. 77–192). Copenhagen, Denmark: Andr. Fred Host & Son.

Olita, A., Sorgente, R., Natale, S., Gaber Sek, S., Ribotti, A., Bonanno, A., & Patti, B. (2007). Effects of the 2003 European heatwave on the Central Mediterranean Sea: Surface fluxes and the dynamical response. *Ocean Science*, *3*, 273–289. https://doi.org/10.5194/os-3-273-2007

Omrani, H., Arsouzeb, T., Béranger, K., Boukthir, M., Drobinskia, P., Lebeaupin Brossier, C., & Maireche, H. (2016). Sensitivity of the sea circulation to the atmospheric forcing in the Sicily Channel. *Progress in Oceanography*, *140*, 54–68. https://doi.org/10.1016/j.pocean.2015.10.007

Onken, R., Robinson, A. R., Lermusiaux, P. F. J., Haley, P. J., Jr., & Anderson, L. A. (2003). Data-driven simulations of synoptic circulation and transports in the Tunisia-Sardinia-Sicily region. *Journal of Geophysical Research*, *108*(C9), 8123. https://doi.org/10.1029/2002JC001348

Ovchinnikov, I. M. (1966). Circulation in the surface and intermediate layers of the Mediterranean. *Oceanology*, *6*, 48–59.

Piccioni, A., Gabriele, M., Salusti, E., & Zambianchi, E. (1988). Wind-induced upwellings off the southern coast of Sicily. *Oceanologica Acta*, *11*(4), 309–314. Retrieved from http://archimer.ifremer.fr/doc/00106/21760/

Pickett, M. H., & Paduan, J. D. (2003). Ekman transport and pumping in the California Current based on the U.S. Navy's high-resolution atmospheric model (COAMPS). *Journal of Geophysical Research*, *108*(C10), 3327. https://doi.org/10.1029/2003JC001902

Pinardi, N., Korres, G., Lascaratos, A., Roussenov, V., & Stanev, E. (1997). Numerical simulation of the inter-annual variability of the Mediterranean Sea upper ocean circulation. *Geophysical Research Letters*, *24*(4), 425–428. https://doi.org/10.1029/96GL03952

Pinardi, N., Lyubartsev, V., Cardellicchio, N., Caporale, C., Ciliberti, S., Coppini, G., . . . Zaggia, L. (2016). Marine rapid environmental assessment in the Gulf of Taranto: A multiscale approach. *Natural Hazards and Earth System Sciences Discussions*, *16*, 2623–2639. https://doi.org/10.5194/nhess-2016-179

Poulain, P. M., & Zambianchi, E. (2007). Surface circulation in the central Mediterranean Sea as deduced from Lagrangian drifters in the 1990s. *Continental Shelf Research*, *27*(7), 981–1001. https://doi.org/10.1016/j.csr.2007.01.005

Powell, B. S., & Leben, R. P. (2004). An optimal filter for geostrophic mesoscale currents from along-track satellite altimetry. *Journal of Atmospheric and Oceanic Technology*, *21*, 1633–1642. https://doi.org/10.1175/1520-0426(2004)021<1633:AOFFGM>2.0.CO;2

Pujol, M. I., & Larnicol, G. (2005). Mediterranean Sea eddy kinetic energy variability from 11 years of altimetric data. *Journal of Marine Systems*, *58*(3–4), 121–142. https://doi.org/10.1016/j.jmarsys.2005.07.005

Rinaldi, E., Buongiorno Nardelli, B., Volpe, G., & Santoleri, R. (2014). Chlorophyll distribution and variability in the Sicily Channel (Mediterranean Sea) as seen by remote sensing data. *Continental Shelf Research*, *77*, 61–68. https://doi.org/10.1016/j.csr.2014.01.010

Rintoul, S. R., Sokolov, S., & Church, J. (2002). A 6 year record of baroclinic transport variability of the Antarctic Circumpolar Current at 140°E derived from expendable bathythermograph and altimeter measurements. *Journal of Geophysical Research*, *107*(C10), 3155. https://doi.org/10.1029/2001JC000787

Rio, M. H., Pascual, A., Poulain, P. M., Menna, M., Barceló, B., & Tintoré, J. (2014). Computation of a new Mean Dynamic Topography for the Mediterranean Sea from model outputs, altimeter measurements and oceanographic *in situ* data. *Ocean Science Discussions*, *11*, 655–692. https://doi.org/10.5194/os-10-731-2014

Rixen, M., Beckers, J. M., Levitus, S., Antonov, J., Boyer, T., Maillard, C., . . . Zavatarelli, M. (2005). The Western Mediterranean deep water: A proxy for climate change. *Geophysical Research Letters*, *32*, L12608. https://doi.org/10.1029/2005GL022702

Robinson, A. R., Sellshop, J., Warn-Varnas, A., Leslie, W. G., Lozano, C. J., Haley, P. J. Jr., . . . Lermusiaux, P. J. F. (1999). The Atlantic Ionian stream. *Journal of Marine Systems*, *20*(1–4), 129–156. https://doi.org/10.1016/S0924-7963(98)00079-7

Roblou, L., Lamouroux, J., Bouffard, J., Lyard, F., Hénaff, M. L., Lombard, A., . . . Birol, F. (2011). Post-processing altimeter data toward coastal applications and integration into coastal models. In S. Vignudelli, A. G. Kostianoy, P. Cipollini, & J. Benveniste (Eds.), *Coastal altimetry* (Chapter 9, pp. 217–246). Berlin, Germany: Springer. https://doi.org/10.1007/978-3-642-12796-0_9

Roether, W., Klein, B., & Hainbucher, D. (2014). The eastern Mediterranean transient: Evidence for similar events previously?. In G. L. Eusebi Borzelli, M. Gačić, P. Lionello, & P. Malanotte-Rizzoli (Eds.), *The Mediterranean Sea: Temporal variability and spatial patterns* (pp. 75–83). Oxford, UK: John Wiley. https://doi.org/10.1002/9781118847572.ch6

Roether, W., Klein, B., Manca, B. B., Theocharis, A., & Kioroglou, S. (2007). Transient eastern Mediterranean deep waters in response to the massive dense-water output of the Aegean Sea in the 1990s. *Progress in Oceanography*, *74*(4), 540–571. https://doi.org/10.1016/j.pocean.2007.03.001

Sammari, C., Koutitonsky, V. G., & Moussa, M. (2006). Sea level variability and tidal resonance in the Gulf of Gabes, Tunisia. *Continental Shelf Research*, *26*(3), 338–350. https://doi.org/10.1016/j.csr.2005.11.006

Sammari, C., Millot, C., & Prieur, L. (1995). Aspects of the seasonal and mesoscale variabilities of the Northern Current in the western Mediterranean Sea inferred from the PROLIG-2 and PROS-6 experiments. *Deep Sea Res., Part I: Oceanographic Research Papers*, *42*(6), 893–917. https://doi.org/10.1016/0967-0637(95)00031-Z

Sammari, C., Millot, C., Taupier Letage, I., Stefani, A., & Brahim, M. (1999). Hydrological characteristics in the Tunisia-Sardinia-Sicily area during spring 1995, *Deep Sea Res., Part I: Oceanographic Research Papers*, 46(10), 1671–1703. https://doi.org/10.1016/S0967-0637(99)00026-6

Schilchtholz, P. (1991). A review of methods for determining absolute velocities of water flow from hydrographic data. *Oceanologia*, *31*, 73–85. Retrieved from http://www.iopan.gda.pl/oceanologia/OC_31/OC_31_73-85.pdf

Sorgente, R., Drago, A. F., & Ribotti, A. (2003). Seasonal variability in the Central Mediterranean Sea circulation. *Annales Geophysicae*, *21*, 299–322. https://doi.org/10.5194/angeo-21-299-2003

Sorgente, R., Olita, A., Oddo, P., Fazioli, L., & Ribotti, A. (2011). Numerical simulation and decomposition of kinetic energies in the Central Mediterranean Sea: Insight on mesoscale circulation and energy conversion. *Ocean Science Discussions*, *8*, 1–54. https://doi.org/10.5194/os-7-503-2011

Stansfield, K., Gasparini, G. P., & Smeed, D. A. (2003). High-resolution observations of the path of the overflow from the Sicily Strait, *Deep Sea Research Part I: Oceanographic Research Papers*, *50*(9), 1129–1149. https://doi.org/10.1016/S0967-0637(03)00099-2

Tsimplis, M. N., & Josey, S. A. (2001). Forcing the Mediterranean Sea by atmospheric oscillations over the North Atlantic. *Geophysical Research Letters*, *28*(5), 803–806. https://doi.org/10.1029/2000GL012098

Vignudelli, S., Gasparini, G. P., Astraldi, M., & Schiano, M. E. (1999). A possible influence of the North Atlantic Oscillation on the circulation of the Western Mediterranean Sea. *Geophysical Research Letters*, *26*(5), 623–626. https://doi.org/10.1029/1999GL900038